PHOTOSYNTHETICALLY ACTIVE ARABIDOPSIS PROTOPLASTS FOR POWER SCAVENGING, ABSORBANCE AND OPTICAL DENSITY ANALYSIS

by

AHMED SHAHID

Presented to the Faculty of the Graduate School of

The University of Texas at Arlington in Partial Fulfillment

of the Requirements

for the Degree of

MASTER OF SCIENCE IN BIOMEDICAL ENGINEERING

THE UNIVERSITY OF TEXAS AT ARLINGTON

May 2011

ACKNOWLEDGEMENTS

"In the name of God, the most Gracious, the most Compassionate" without him nothing is possible. I would like to thank Dr. Samir M. Iqbal for giving me an opportunity to work in his lab and polish my skills in many fields. He has always been an excellent mentor throughout my research assistantship under him. He has given wonderful opportunities to many struggling students and has always been there to guide and encourage me to seek more and more. I have learned a great deal of knowledge as a student and a researcher by working with Dr. Iqbal.

I also would like to thank Dr. Maeli Melotto for her marvelous help, directions, and support during this project. She provided me access to her lab and also provided me with most of the apparatus along with the chemicals that were prepared during this research. I would also like to acknowledge Dr. Melotto's group members for providing me friendly environment in the lab and for helping me during this project. I would also like to thank Dr. Michael H. – C. Jin and his group for helping and training me with the equipment in their laboratory.

I would also like to thank my friends and coworkers for their help and support during the project and our Alumni students of Nano – Bio lab who helped me during my first semester. I would also like to acknowledge the staff of Nanotechnology Research and Teaching Facility for their assistance and help while working in cleanroom and even outside.

Last but not least, I would like to thank my family for their continuous support, financially and emotionally and for understanding my priorities towards education.

April 15, 2011

ABSTRACT

PHOTOSYNTHETICALLY ACTIVE ARABIDOPSIS PROTOPLASTS
FOR POWER SCAVENGING, ABSORBANCE
AND OPTICAL DENSITY ANALYSIS

Ahmed Shahid M. S.

The University of Texas at Arlington, 2011

Supervising Professor: Samir M. Iqbal

Plants and photosynthetic bacteria hold protein molecular complexes that can efficiently harvest photons. This thesis presents fundamental studies to harness photochemical activities by converting photonic energy into electrical energy. The electrical behavior of protoplast extracted from *Arabidopsis* plants was characterized in the presence and absence of light. The photo-induced reactions of photosynthesis were measured using a patch clamp measurement system at a constant voltage. The absorbance and optical density measurements showed very large bandwidth for extracted protoplasts. The optical measurements were performed on the protoplast of *Arabidopsis* thaliana plants and showed absorption bands at a number of wavelengths. The analysis of the optical data showed that proteins complexes obtained from photosynthetic cells can overcome the limitation of traditional organic solar cells that cannot absorb light in the visible- Near Infrared (NIR) spectrum. The current-voltage measurements done on protoplast extracts showed two orders of magnitude change when exposed to light. The demonstration of electrical power scavenging from plant

from plant protoplast can open avenues for bio–inspired and bio-derived power with better quantum efficiency.

TABLE OF CONTENTS

LIST OF ILLUSTRATIONS

LIST OF TABLES

CHAPTER 1

PROTOPLAST FOR EFFICIENT ENERGY CONVERSION DURING PHOTOSYNTHESIS

1.1 Introduction

Natural systems have very efficient energy carrying and conversion capabilities. The processes involved in the conversion of photonic energy into electrical energy have thus attracted considerable attention since the 70s [1]. In the past few decades a lot of work has been focused on various applications of photosynthetic proteins in technology, ranging from light-induced electron transfer, sensing of herbicides, hydrogen production, etc. [2-5]. There are fundamental limits in harnessing photochemical activities that have hampered the use of natural systems in meeting the energy needs of humans. With ever-increasing use of energy, the sources of energy are becoming over-burdened and depleted. The urgency for more efficient alternatives and renewable energy sources cannot be over-emphasized. With an immense increase in the atmospheric concentration of green-house gases emitted by the use fossil fuels, it is important to develop non-conventional fuels. However, environmental safety becomes a core concern when discussing alternative energy. Therefore, the use of organic molecules instead of chemicals is attractive and has gained a lot of attention in research. The spectrum of electromagnetic radiation striking the Earth's atmosphere is from 10^2 to 10^6 nm. Ultraviolet (UV) radiation (100 – 400 nm) is mostly absorbed by the atmosphere and very little reaches the Earth's surface. Visible light spans over 400-780 nm whereas infrared (IR) spectrum extends from 700-$5x10^5$ nm. Visible-near IR (NIR) region (400–1000 nm) corresponds to more than 70% power of solar radiation [6] and the conventional organic solar cells are not capable of absorbing light in this region due to their large bandgaps. Most organic semiconductors have bandgaps higher than 2 eV that limits the absorbed spectrum to <600 nm and can possibly

absorb only 33% of solar radiation [7]. This work focuses on using a natural resource, i.e. plants that has evolved into the most efficient energetic systems to capture solar radiation, the most abundant source of energy on Earth, as an alternative energy source.

1.2 Solar Energy and its Applications

Solar energy, a carbon-neutral energy source, is the ultimate and reliable key to the energy and environmental challenges. Various applications of solar energy have been aggressively pursued during the last few years. Various studies have focused on improving energy conversion efficiencies and development of organic solar cells in order to design organic devices making use of light-induced electron transfer [2, 7-9]. Organic solar cells have quite a few advantages over traditional inorganic solar cells due to much lower production cost, flexibility and large area applications; however, the traditional organic solar cells have the limitation of not being able to absorb light in the visible and NIR region that make up the majority of the power (over 70%) of total solar radiation [6]. Plants and photosynthetic bacteria contain molecular complexes that can efficiently harvest photons and overcome these limitations by absorbing light in the visible-NIR range (400-1000nm). Photosynthetic reaction centers harvest photons with a quantum yield of greater than 95% [10, 11]. The work on photosynthetic proteins in light-induced electron transfer and hydrogen production, [3-5] can directly contribute towards achieving an alternate source of energy in a cleaner and greener fashion. The basic step for converting energy, solar energy, to another form, electricity or biomass can be described by the essential processes as, each photon absorbed by the light an electron is promoted to the higher energy level, or excited state. This promotion of an electron leads to an excited state in which an electron is repositioned in spatial and the energy coordinates. In the process, it leaves a positive charge behind. In other words, the electron is reduced and the positive charge left behind is chemically oxidized. The sun light is absorbed by the photosynthetic antenna. Antenna later transfers the excited electron, excitation energy, to the reaction center. There are two types of antenna, a core antenna complex and the peripheral

antenna complex [12]. In this thesis, we demonstrate an approach to capture and use photosynthetic protein complexes for photo-to-energy conversion, extracted from *Arabidopsis* plants.

1.3 Photosynthesis

Photosynthesis is very important process by which plants, some bacteria, and some protistans use the energy, delivered by sunlight, to produce sugar. The plants usually found on the surface of earth have plenty of sunlight that is converted into sugar which is then converted by cellular respiration into ATP, a source of energy for any living being. However, these plants do not utilize all the photons they absorb from sunlight. In photosynthetic organisms, most of the sunlight is absorbed by the antenna pigment protein complexes, rather than by the reaction center that converts excitation energy to electrochemical potentials [13]. As discussed in the previous section, plants and photosynthetic bacteria contains protein complexes that can efficiently harvest photons and overcome the limitations by absorbing light in visible NIR range. Photosynthetic reaction centers harvest photons with quantum yield of greater than 95 % [10, 11]. The Bis-Phenyl-Ethynyl Anthracene (BPEA) antenna features absorbance maxima at 309, 319, 445, and 469 nm and emission maxima at 483.52 nm and ~547 nm [13]. As described in section 1.2, the sun light is absorbed by the antenna systems in plants which are also called as photosynthetic antennas which later transfer the excited electrons, excitation energy, to the reaction center. There are some species which capture very minimal sunlight but are able to use most of it to complete the process of photosynthesis and respiration that is essential for plants to survive. In design and construction of artificial photosynthetic complex, for solar cell, the antenna systems are in interests. In synthetic molecules use the basic photochemistry and photo – physics of photosynthesis to carry out solar energy conversion [13]. These species are discussed in detail in Chapter 2. The basic schematic of photosynthesis light reaction and respiration process is shown in Figure 1.1.

The basic photosynthesis equation in presence of light is given as:

$$CO_2 + 6H_2O \rightarrow C_6H_{12}O_6 + 6O_2$$

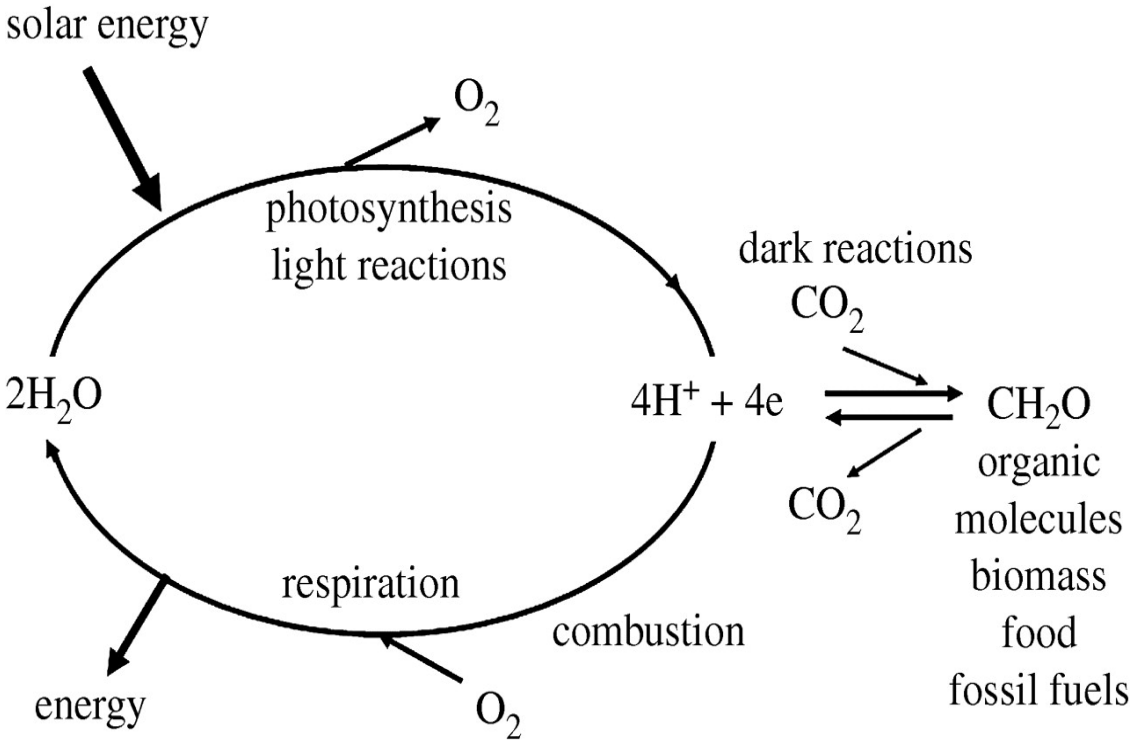

Figure 1.1 The flow of energy in plants [14].

CHAPTER 2

LITERATURE REVIEW

2.1 *Chlorobium Limicola*

Chlorobium limicola also known as green sulfur bacteria (GSB) has markedly different photosynthetic thrusts cross – cut the two goals of electrical energy generation. *Chlorobium limicola* is mostly present in deep water species where sunlight hardly reaches. This plant captures tiny amount of light and uses most of it to complete the process of photosynthesis essential for this plant to survive. It contains two distinct antenna chlorophylls; bacteriochlorophyll c and bacteriochlorophyll a (BChl c, BChl a) [17]. The ratio of these antennas to the reaction center is an order of magnitude greater than that in other chlorosomes and of purified fraction of cytoplasmic membrane and has provided information on the location of the different chlorophylls within the cells [17]. In natural habitats, both light energy and light quality change as a result of physical properties of water, chemicals in solution, suspended particles, and biological filtering by phototrophic microorganisms [15]. It has been demonstrated in the laboratory that green and yellow light is selective agent for enrichment of purple sulfur bacteria whereas blue light favors growth of green sulfur bacteria [16, 17].

According to the most of the literature that is present to date for *Chlorobium limicola,* it is believed that *Chlorobium limicola* and its efficiency to convert very little amount of light that reaches it, its ability to complete the photosynthesis and respiration cycle is remarkable. The structural model of *Chlorobium limicola* chlorosome and cytoplasmic membrane is shown in Figure 2.1. *Arabidopsis* was used as a model system to isolate protoplast and to verify and benchmark the efficient conversion of photo-energy, the bacterial PS I core and outer antenna

system was isolated. *Arabidopsis*, its method of, isolation, measurements, and results are discussed in later chapters.

2.2 Function and Efficiency of *Chlorobium Limicola*

In the photosynthetic process of green sulfur bacteria light energy is transferred to the reaction center in the cytoplasmic membrane by the antenna system, the antenna system is called chlorosomes [17]. The photosynthetic reaction center captures light to an effective level with 200,000 bacteriochlorophylls (BChl a, c, d, or e) per chlorosome [17]. The BChl c, d, or e present in the chlorosomes, are arranged in tubular stacks with absorption at 720 – 750 nm [17]. To prepare the reaction center polypeptides Fenna – Mathews – Olson BChl (PscA – D plus FMO, a protein) is involved. In *Chlorobium limicola*, there are 21 histidines per PscA present and the energy transfer of chlorophyll in very efficient in P840 reaction center as compared to any other cartenoids studied. Also, the rate of electron transfer in P840 reaction center has a potential of approximately 240 mV [17]. The reaction center of GSB, contained in *Chlorobium limicola*, is shown in Figure 2.2.

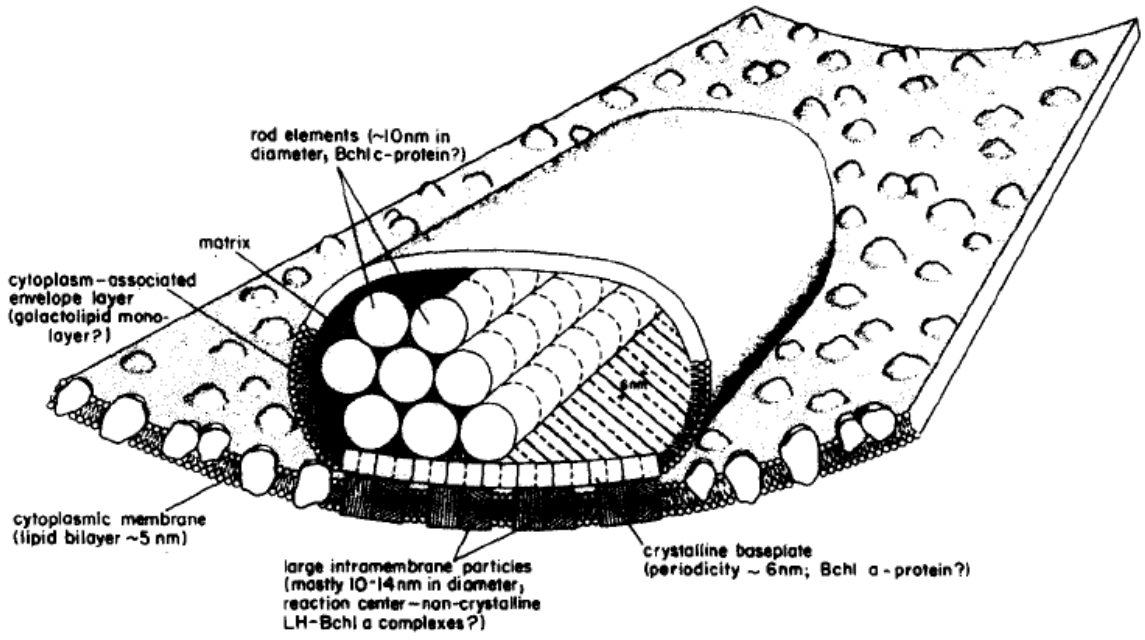

Figure 2.1 Structural model of *Chlorobium limicola* chlorosome and cytoplasmic membrane [18].

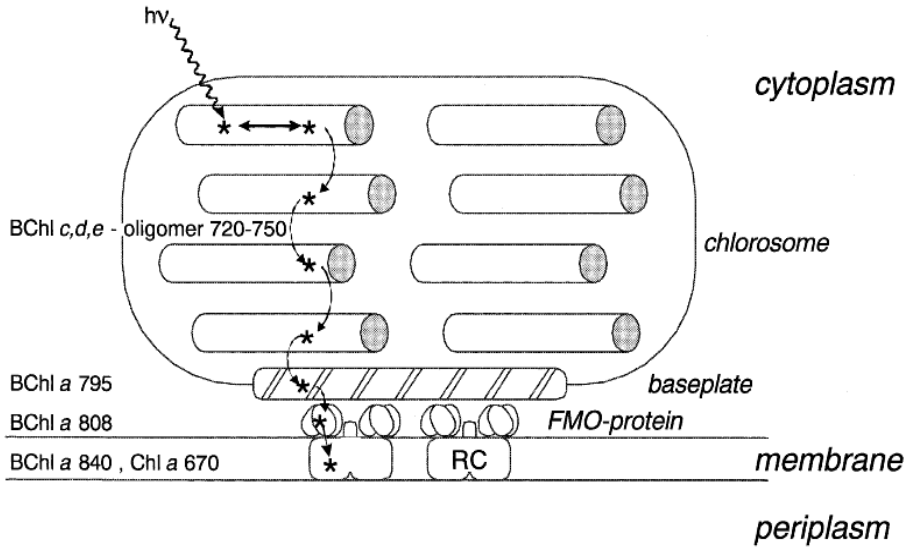

Figure 2.2 The reaction center of green sulfur bacteria [17].

2.3 Protein Complex in Plants

In higher plants, cyanobacteria, or algae there is a chloroplast which consists of photosystem I and photosystem II, which are the main parts of photosynthesis in them. The photosystem has core complex and the peripheral light harvesting complex (LHC) [19]. Chlorophyll a that contains core complex in thylakoid membrane of photosystem I (PS-I) captures solar energy and delivers the excited electrons to the reaction center (RC) where it is converted into electrochemical energy [6]. In a biomimetic system, it is not enough to duplicate the solar conversion ability of chlorophyll, but rather systematic approaches are required to efficiently interface the RC and the pigment – protein complexes, that trigger the photochemistry for unidirectional electron transfer. It is widely believed that the PS I core organization applies to all iron sulfur reaction centers [20]. The PS-II is a multienzymatic chlorophyll protein complex in the thylakoid membrane of bacteria, algae and higher plants [3]. The use of PS-I was advantageous in the applications to measure the electron transfer from PS-I to reaction center which was shown by using *Arabidopsis* as a benchmark.

2.4 Quantum Yield of Reaction Centers

The chloroplast consists of PS-I and PS-II and protoplast contains the chloroplast. PS-I is a supramolecular protein complex that drives photosynthesis. For energy transfer process it is important to know the distance between the antenna systems aligned to make the antenna network which is connected with the help of monomeric chlorophylls in the reaction centers [22]. PS-I, with the molecular weight of ~ 300 kDa, exhibits a quantum yield of around 1 that generates photoinduced charged separation within 3 – 10 ps across 6 nm length. The quantity and the concentration of the photosystems are measured spectrophotometrically by subtracting dark absorbance difference at particular frequencies from light [23]. To measure quantum yield, the light saturation curve of photosynthesis are measured to determine the efficiency (quantum yield) and productivity of photosynthesis. PS-I is a transmembrane protein complex to which photoexcited electrons travel via an electron transport chain (ETC) in the membrane. The process of photosynthesis that involves PS-I, PS-II, and ETC is shown in Figure 2.3.

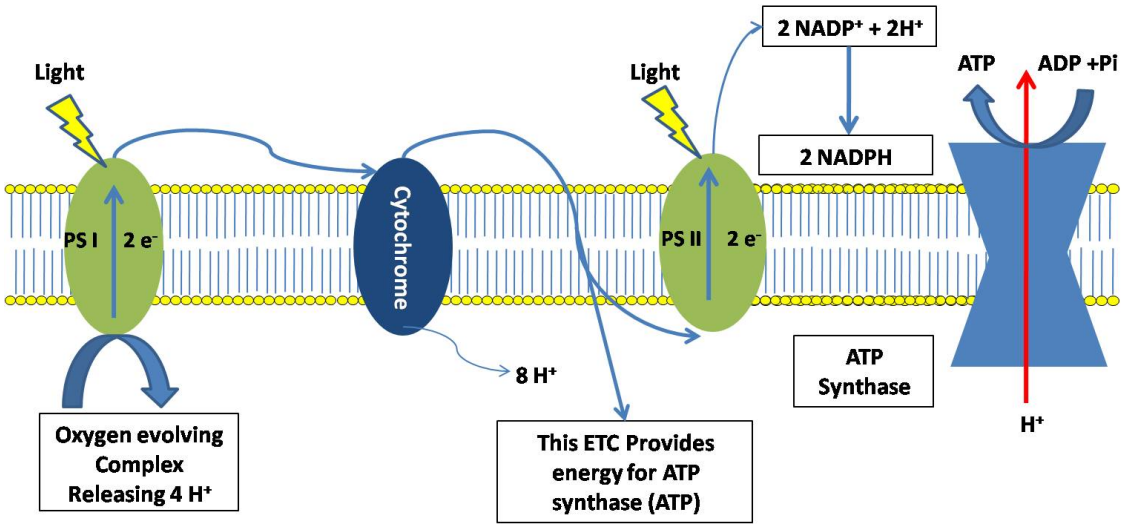

Figure 2.3 Schematic of how electron is transported from PS I to PS II, electron transport chain (ETC) in a light dependent reaction.

CHAPTER 3

LITERATURE REVIEW

3.1 Background

Arabidopsis thaliana, an angiosperm, is one of the most widely used plants for the study of a broad range of problems in areas involving development, metabolism, genetics, environmental adaptation and pathogen interactions [24]. Arabidopsis belongs to the mustard family *Brassicaceae* (also known as *Cruciferae*) which is an extensively distributed family of approximately 340 genera and approximately 3350 species [9]. Although of no inherent economic significance, Arabidopsis with its small size, rapid life cycle, small simple genome, prolific seed production and the accessibility of numerous mutant plant lines puts forward various advantages for rapid genetic and molecular analysis. This weed is generally self-pollinated and takes only 5 – 6 weeks from seed germination to the production of a new generation of seeds. It has thus turned out to be the focus of the first plant genome project to study the biology of a flowering plant at the molecular level [9]. In this work, *Arabidopsis* was used as a model system as a proof of concept that organic cells are more efficient that traditional inorganic cells. The protoplast (cells without the cell walls) from *Arabidopsis* was isolated to study the photonic to electric conversion efficiency of the photosynthetic protein complexes.

3.1.1 Growing Arabidopsis

The choice of Arabidopsis is to verify and benchmark the isolation of bacterial PS1 core and the outer antenna (PS-I – LHC1) components. In order to grow the plant, a soil mixture consisting of growing soil medium (Redi-earth plug and seedling mix, Sun Gro, Bullevue, WA), fine vermiculite, and perlite in 1:1:1 (v:v:v) was prepared. The mixture was filled in three-inch

plastic pots soaked with water. 100 ml of gnatrol was added in an autoclaved soil to prevent fungus contamination, which was observed in the past. Autoclaving the premixed soil resulted in slowed moistening of the soil. It normally took around 24 hours for soil to be moist once the pots were settled in a big flat and filled 1/8 with water but, because of autoclaving, the moist soil was observed after 48 hours instead of 24 hours. While making the pots, mask cover was used as vermiculite is fatal for lungs. Vermiculite is a micaceous mineral that expands on heat treatment. Vermiculite has many uses in construction industries, agriculture, and packaging [25]. After 48 hours when the soil was moist, it was covered with a layer of moist vermiculite and finally covered with a mesh. Pots covered with vermiculite and mesh covers are shown in the Figure 3.1. After covering it with the mesh, seeds were sown using a seed suspension in 0.1 % agarose (Columbia (Col-0), ABRC stock Center, Ohio). During the sowing process, there were five points only where the seeds were sown, to have controlled growth and reduce the waste of seeds. After the flat had all the pots covered with mesh and sown with seeds, the pots were labeled (Col-0), covered and kept under a temperature of 4 ^{0}C for two days. This cold treatment helps synchronize the germination seeds. The pots were moved to a growth chamber and kept at the environmental conditions. Figure 3.2 show the pots in growth chamber. The growth chamber had 22 ^{0}C, 60±5 % relative humidity, and a 12 hour photoperiod under light intensity of 100 ìmol·m^{-2}·s^{-1}. After 2 weeks the leaves started growing and eventually the plants were fully expanded leaves. These fully grown plants (4- 6 weeks) were used for protoplast isolation. The Figure 3.3 shows growth of Arabidopsis at different development period, the progress in two weeks and the growth progress in full 4 weeks is shown in Figure 3.4.

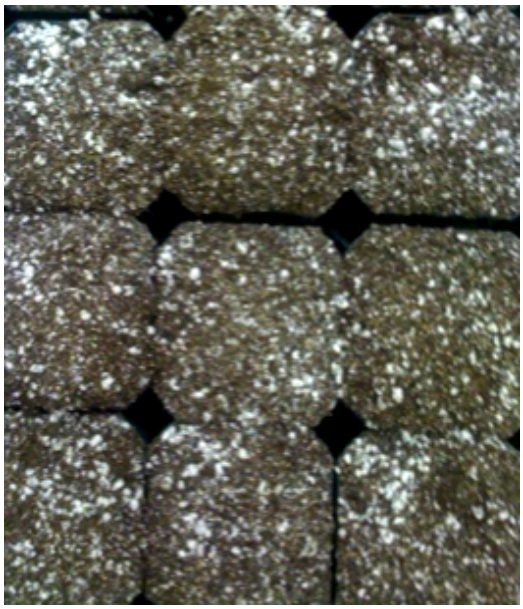

(a)

(b)

Figure 3.1 (a) Mixed soil pots soaked in water and fungicide (b) Pots with moist soil and covered with mesh.

Figure 3.2 Pots with mixed soil and sown with seeds were placed in growth chamber.

Figure 3.3 Growth of *Arabidopsis* at different stages of development (starting from left, week 1 – week 3) after sowing.

Figure 3.4 Growth of *Arabidopsis* in four weeks after sowing.

3.1.2 Isolation of Protoplast from Arabidopsis

When the cell wall of plant, bacterial, or fungal cell is removed completely by some enzymatic means or reactions, it is called protoplast. The isolation of protoplast was performed in house using the adapted protocol [26-28] with slight modifications. The modified protocol was; approximately 50 young leaves with good size and color were plucked carefully and blended together with 100 ml of water for 5 minutes. After 5 minutes the blended solution was filtered using a 100 µm nylon mesh. The residues, which consisted of epidermal and mesophyll cells, were transferred to a flask that contained a mixture of 500 µl of 0.7 % cellulysin, 50 µl of 0.01 % Poly – vinyl – pyrrolidone (PVP), 500 µl of 0.25 % Bovine Serum Albumin (BSA) and 2.75 ml of 55 % basic medium (0.5 mM $CaCl_2$, 0.5 mM $MgCl_2$, 5 mM MES, 500 mM D-sorbitol). Then the mixture was incubated in dark for 3 hours under 25 ^{0}C, at 100 RPM (using Labnet orbit 1000, ~0.45 xg) and filtered again through 100 µm nylon mesh. The residue was collected in a flask containing a mixture of 500 µl 1.5% cellulose, 500 µl 0.03 % Pectolyase, 500 µl 0.25 % BSA and 2.95 ml Basic medium. This mixture was incubated in dark for 2 hours at 18 ^{0}C with a speed of 0.38 xg (~70 RPM using Labnet orbit 1000). After incubation the mixture was filtered through four nylon meshes (pore size = 100 µm) and the filtrate was collected in a tube. The

tube containing filtrate was centrifuged at 1000 xg for 5 minutes (using Centrifuge 5810R – Eppendorf). The supernatant was passed again through the same four layers of nylon mesh and centrifuged again at 1000 xg for 5 minutes and this process was repeated twice to isolate the protoplast. The structure of protoplast suspension was further examined. The structure of protoplast suspension is shown in Figure 3.5 and Figure 3.6. Protoplast structure is observed to be ~ 100 µm. To observe the structure closely Figure 3.7 was captured during examination. The total volume of protoplast suspension obtained was ~ 1.6 ml which is shown in Figure 3.8 used for further observations.

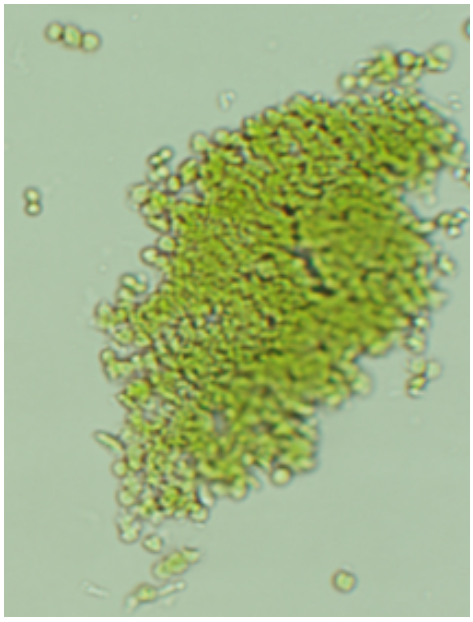

Figure 3.5 Protoplast suspension isolated from *Arabidopsis* plants.

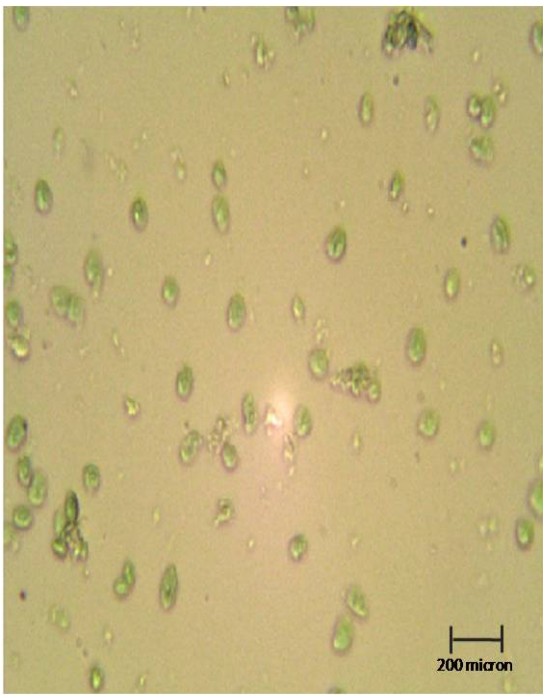

Figure 3.6 Protoplast suspension isolated from *Arabidopsis*, showing the structure of healthy cells.

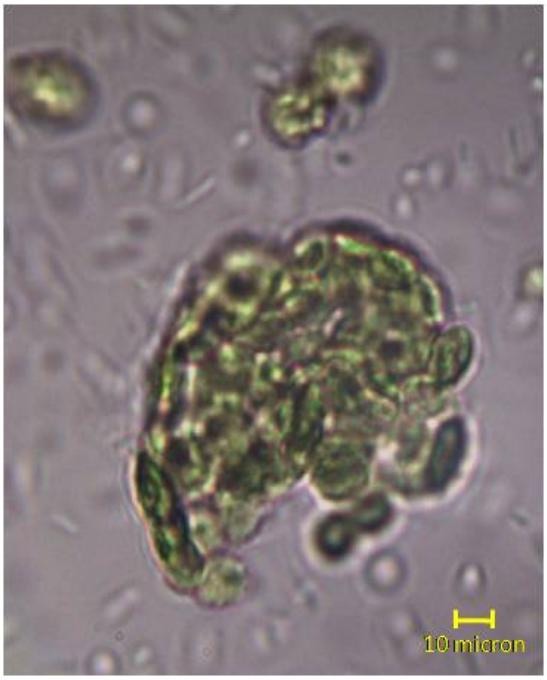

Figure 3.7 Magnified image of extracted protoplast.

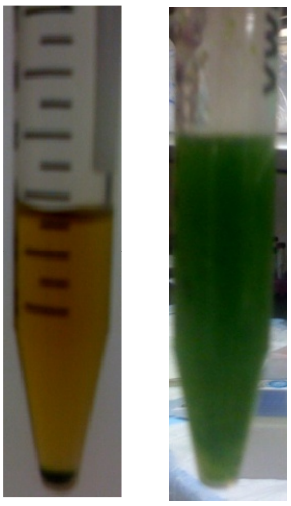

Figure 3.8 Protoplast sample extracted from approximately 50 leaves, the sample collected was around 1.6 ml. The figure on the left is sample collected after final filtration and right figure shows sample without any filtration.

3.1.3 Preparation of Protoplast for Experiments

The measurement system was housed in an electrically and magnetically shielded enclosure placed on vibration-isolation table. The extracted protoplast was stored in dark between 4–10 ℃. The protoplast consisted of live cells and these could easily die in case of too much light or heat exposure. The protoplast suspension was observed under microscope to make sure that 90 % of the cells were approximately size of 100 µm. Before the experiments, protoplasts were inspected under the microscope to make sure that they were alive as indicated by the integrity of the cells and organelles. For the very first few measurements, buffer solution 1, buffer solution 2, and protoplast suspension were analyzed side by side to make sure that the current produced was not from any of the buffer solutions. Buffer solution 1 was completely washed off during the experimental process, but it was thought to be necessary to test it as well. Once it was confirmed that buffer solution 1 had no effect on generation of current, it was eliminated from later experiments and analysis. The extracted protoplast and buffer solution were stored at 4 ^{0}C for later use.

3.2 Measurements

All the measurements discussed here were performed many times (14 times). Each independent experiment performed during this project, the protoplast was isolated from the plants and the buffer solutions were prepared for each independent experiment separately as well. The protocol used for all the experiments was exactly the same as discussed in previous section. The equipments used for measurements (*I-V* Measurements and Optical Density) are shown in Appendix B.

3.2.1 Measurements Using LabVIEW Integrated with Patch-Clamp

LabVIEW software was designed to provide constant voltage and measure current produced by the extracted PS1 and LHC1 present in protoplast suspension. The schematic of LabVIEW program designed for the experiments is shown in Figure 3.9. Figure 3.10 shows the front end window of LabVIEW program in which user can select various tasks and save the output data into desired format and location. Axopatch 200B, an amplifier with low-noise patch clamp recording which is used for single channel recordings with minimized signal to noise ratio, was used at a variable voltage supplied. The data was measured with Digidata 1440A, LabVIEW, and analyzed with pClamp software. The electrodes were dipped in the first buffer solution and it was kept under dark to measure the current produced when the voltage supplied was increased from 0 to 75 mV with step size of 1 mV per millisecond. Then the electrodes were changed and the protoplast suspension and buffer solution were kept under the light for the measurements under the same conditions and voltage range. The current measured from PS-I – LHC1 solution was observed and interesting results were obtained which are discussed under results. The responses that were observed for protoplast suspension and buffer solution during this process were used for statistical analysis. The basic schematics of how the systems were connected and measurements were recorded is shown in Figure 3.11.

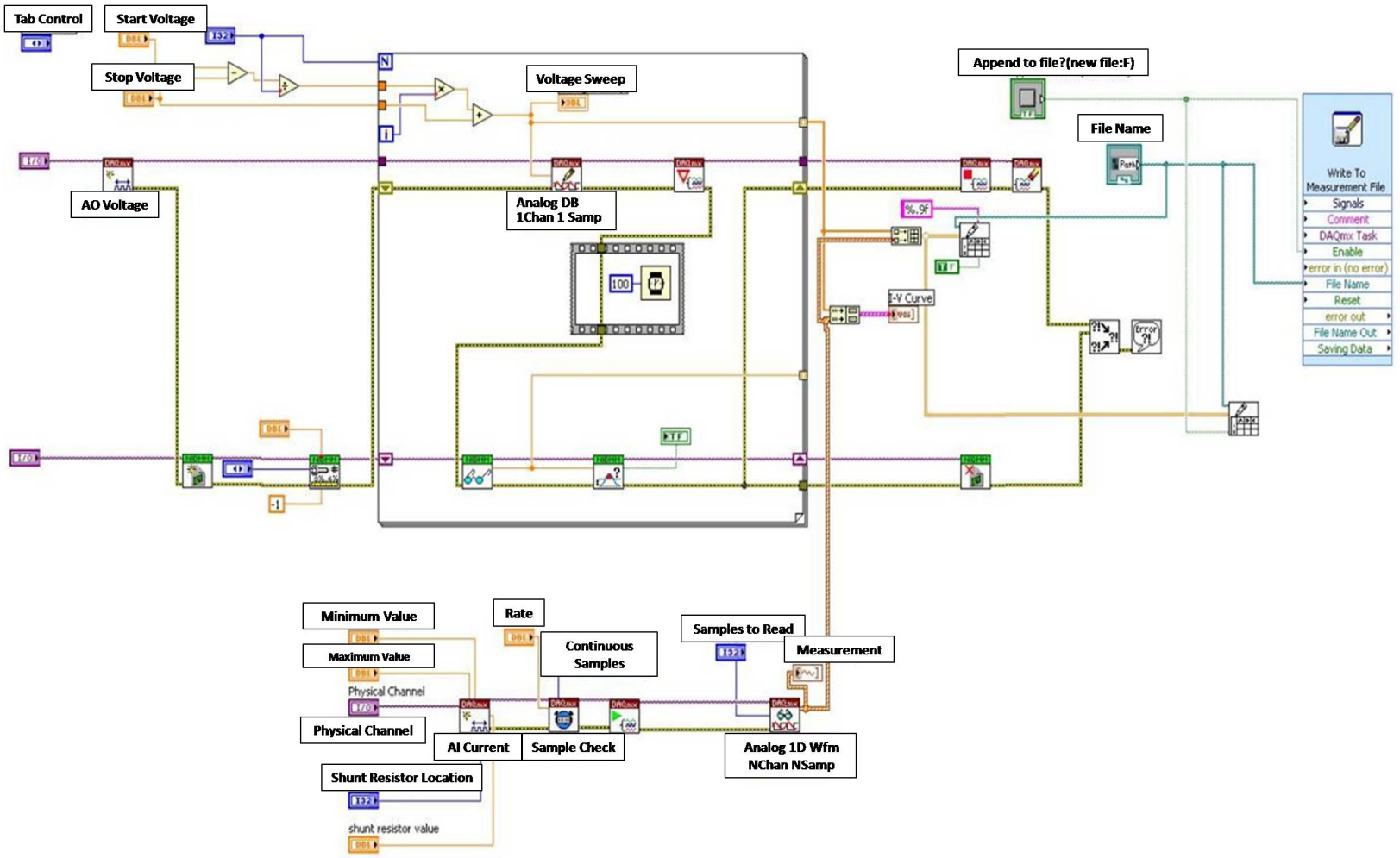

Figure 3.9 Block view of the program designed in LabVIEW for *I-V* measurements.

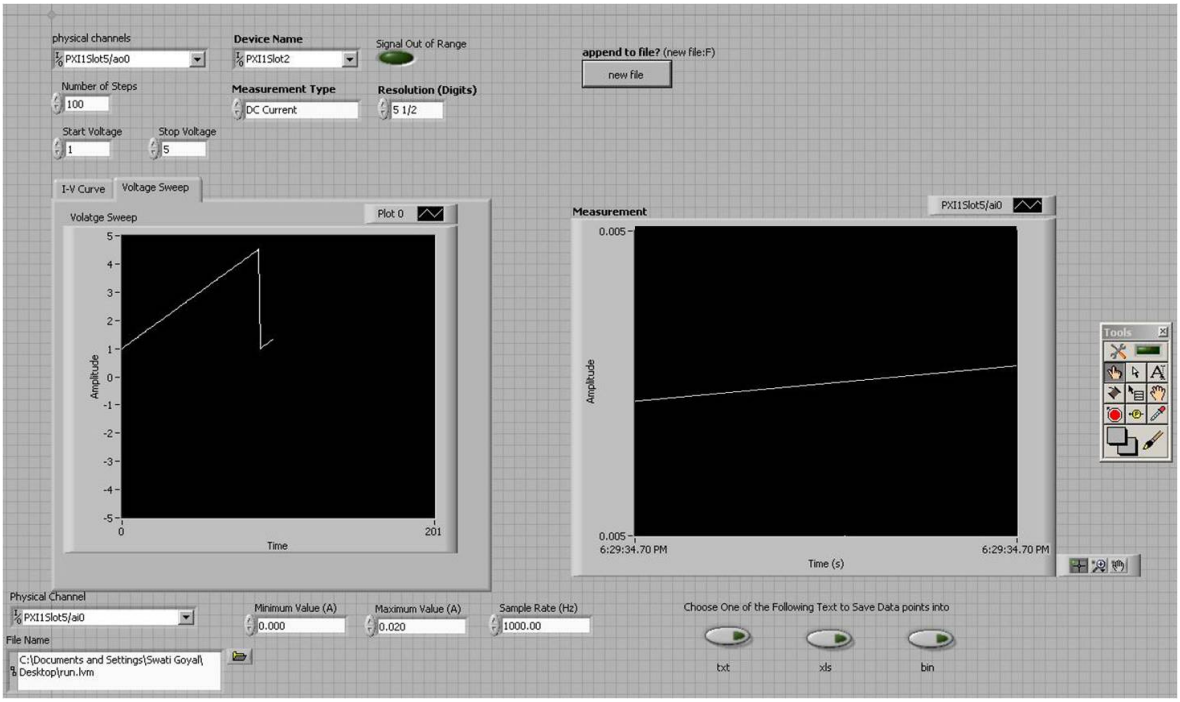

Figure 3.10 Front end GUI of the program designed for *I-V* measurements. The voltage was swept from 0 to 75 mV.

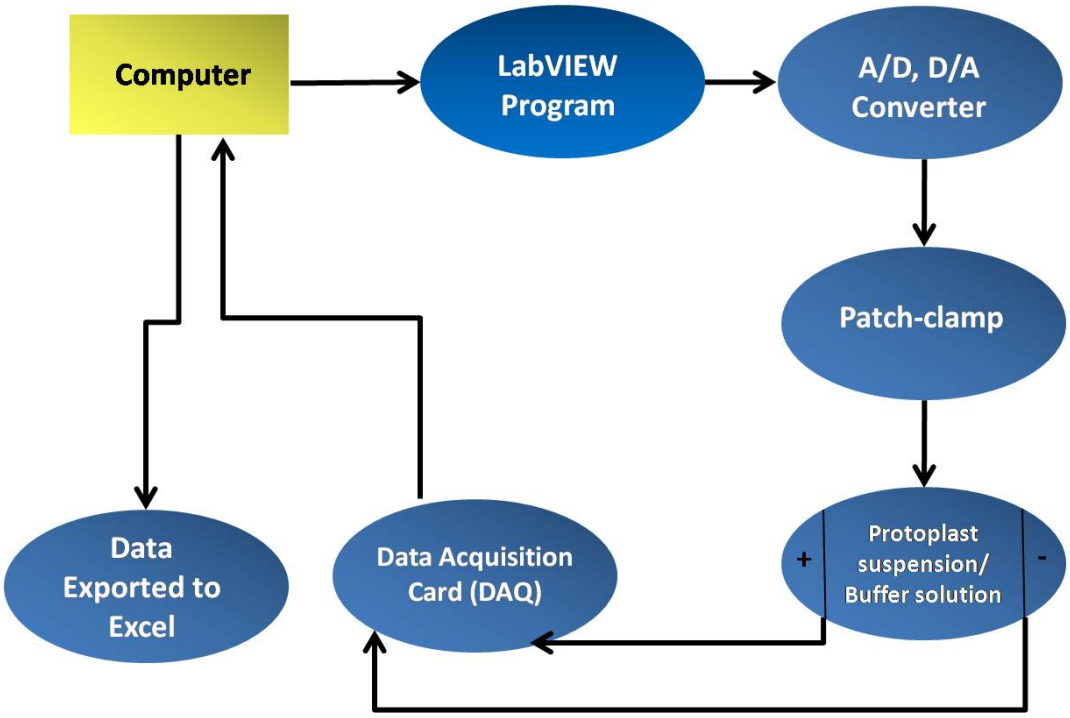

Figure 3.11 Schematics of the systems connected for measurements.

3.2.2 Current – Voltage Measurements

For Current–Voltage (*I-V)* measurements, a different setup was used in order to confirm the results obtained using LabVIEW and Axopatch 200B. *I-V* probe station was used to acquire measurements when voltage was swept between 0-75 mV. The conditions for probe station were kept same as when LabVIEW and patch clamp setup. The response of the protoplast suspension and buffer solution was observed to be similar to the response achieved using method discussed in 3.2.1 under the same conditions. These conditions are explained in detail in later sections. Figure 3.12 is an example of sample run generated during *I-V* measurements using probe station.

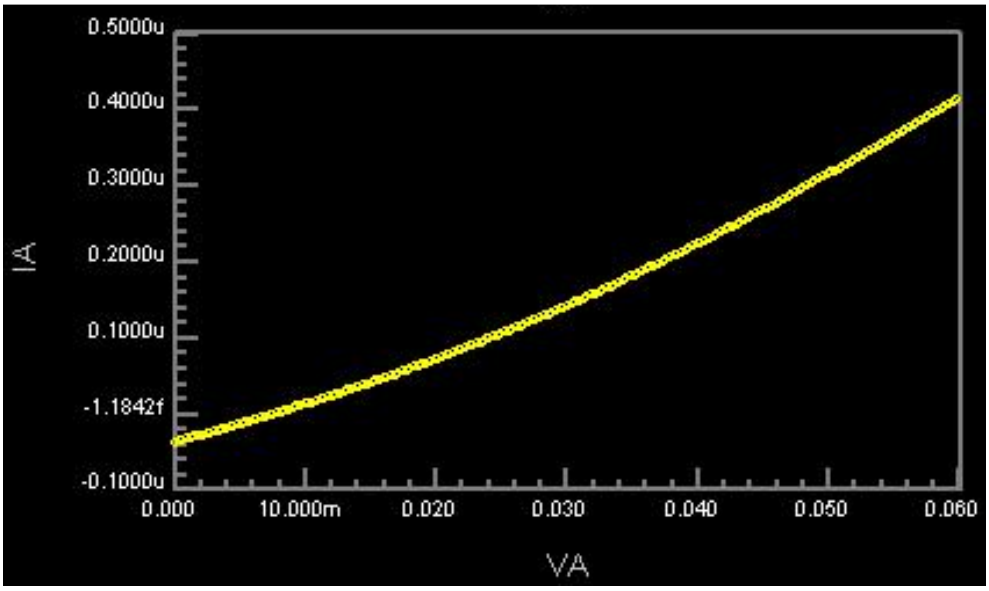

Figure 3.12 Data measured with IC Lite software from Probe Station.

3.2.3 Optical Density Measurements

The protoplast extract of Arabidopsis was characterized for its optical absorbance. The protoplast (called the sample) and the buffer solution absorbance were measured with a spectrophotometer (Perkin Elmer UV/VS/NIR spectrometer). UV WinLab Software was used to calibrate the system. The range of wavelength was chosen to be 300–1000 nm. Three

different measurements (protoplast suspension, buffer solution and the empty cuvette) were processed under the same conditions.

The data of the empty cuvette and the buffer solution was used for background subtraction. The experimental measurements were collected in terms of transmittance (*T*) which is the ratio of light intensity after it passes through a certain sample. The relationship between the absorbance (*A*) and transmittance (*T*) is defined as:

$$A = - LOG (I/I_0) = - LOG (T) \textit{ or}$$

$$A = (-LOG(1-(Transmittance/100)))$$

This relation is well known as Beer-Lambert Law which states that, "*absorption is proportional to the concentration of absorbing species in the material"* [29]. Absorbance, in spectroscopy, is also known as optical density and has no units has no unit and A.U is written for units. An increase of 1.0 AU means that the transmittance is reduced by a factor of 10.

The calculated data for absorbance indicate peaks at certain wavelengths, which are shown in Table 3.1. These peaks indicate higher absorbance at certain wavelengths.

Table 3.1 Peak intensity of absorbance: Comparison of buffer solution and protoplast suspension.

Percent absorbance by protoplast suspension	**Peak Wavelength λ (nm)**
18.71	669
48.82	340
Percent absorbance by buffer solution	**Peak Wavelength λ (nm)**
None	None

3.2.4 Optical – Electrical Characterization

The Arabidopsis protoplast was used for optical-current conversion measurements. As control, *I-V* measurements through protoplast suspension were taken in the dark and under light. All the samples were tested several times under the same conditions. A LabVIEW program was developed interfacing a digital multimeter for measurements. The current was

measured at fixed as well as ramping applied voltage from 0 to 75 mV. Figure 3.11 shows a block diagram of the measurement system. After system calibration, 0.8 mm diameter Ag/AgCl electrodes were used to measure electrical data. The buffer solution was used as control. Ag/AgCl electrodes were used to measure electrical data. The buffer solution was used as control.

3.2.5 Problems Encountered During Measurements and Device Limitations

During the experiment, 100 mV was supplied generating current that was beyond the system's threshold of 200 nA. Axopatch (Axon 200 B) was used to observe the behavior of these samples. Generated current that was more than the system's limitations signaled that the system is overloaded. After observing the same pattern during a few experiments, it was safe to conclude that the current generated is a little more than 200 nA. To overcome the limitations, LabVIEW software was used after calibrating it with a DMM system. The DMM chase board was connected to a DAQ-68 card using NI – 6070E card. One of the drawbacks of using LabVIEW is that it can pick up noise generated by surrounding environment i.e., air pressure and room temperature etc. However, the data generated clearly indicates the difference between the output current generated in protoplast with the light exposure and without it. As every system has its drawbacks, it is very difficult to achieve ideal environment for any measurement. Close observation of measurements using copper electrodes concluded that there was a chemical reaction between the copper and the buffer solution. After further studies of the reactions, it was determined that buffer solutions, including chemicals like oxygen, calcium chloride, magnesium chloride, and hydrogen, reacted with the copper electrodes. The experiments were later repeated using silver coated electrodes in place of copper electrodes. The possibilities of the chemical reactions are:

$$2\ Cu + O_2 \rightarrow 2\ CuO \quad (1)$$

$$Cu + 4\ N_2O_4 \rightarrow Cu\ (NO_3)_4 + 4\ NO \quad (2)$$

$$MgCl_2 + Cu \rightarrow CuCl_2 + Mg^{2+} \quad (3)$$

$$CaCl_2 + Cu \rightarrow CuCl_2 + Ca^{2+} \quad (4)$$

$$Cu + H_2O \rightarrow CuO + H_2 \quad (5)$$

Among the above-mentioned reactions, it is believed, the reactions that are most likely to occur are reaction 3 and reaction 4 due to a strong liking between chlorine and copper. Further properties of Halogen and other families are explained in detail [30]. After observing the reactions, the electrodes were changed from copper to silver (with 0.8 mm dia. x 8 mm Ag/AgCl) electrodes. Buffer solutions were used as controls to test protoplast suspension extracted from *Arabidopsis*.

3.3 Results

3.3.1 Isolated Protoplast

The process of isolation of protoplast took approximately 10 hours. The experiment was repeated 14 times and all data showed similar trend. It is very important to observe the structures of protoplast carefully before measurements. The structures observed in Figure 3.5 and Figure 3.6 are ideal for measurements. The structure shown in Figure 3.7 is extracted protoplast solution after 10 days. The sample however was still usable but not recommended because the protoplast shrinks and eventually dies due to lack of nutrients required to survive. Figure 3.8 shows the total volume (~ 1.6 ml) of sample collected from 50 young leaves. Again, it is very important to choose young leaves and they should neither be stressed (wrinkled texture) nor dried out (leaves turns yellow).

3.3.2 Current Voltage (I-V) Measurements

The density of protoplast per ml was calculated using hemocytometer. The experiment was performed 14 times and the average density was ~ 1.96 x 10^6 (protoplast per ml). The density of each experiment calculated is shown in Table 3.2.

Table 3.2 Densities of protoplast suspended in buffer solution for all the experiments performed independently.

Experiment #	Density (protoplast/ml)	Experiment #	Density (protoplast/ml)
1	1.66×10^6	8	2.01×10^6
2	1.86×10^6	9	2.11×10^6
3	1.89×10^6	10	1.96×10^6
4	1.98×10^6	11	1.95×10^6
5	1.87×10^6	12	2.20×10^6
6	1.84×10^6	13	1.85×10^6
7	1.99×10^6	14	1.83×10^6

3.3.3 Current Voltage (I-V) Measurements

The results of the samples, buffer solution and protoplast suspension, as the voltage was swept between a range of 0 – 75 mV, were studied for current generation. The electrical response of the plain buffer solution with and without light is shown in Figure 3.13. The plot shows that when the electrical potential was applied through the buffer in dark, the current increased linearly as a function of voltage and it was ~10 nA at 75 mV. When the same experiment was repeated in the presence of light, it showed a slightly higher current in the same order. The experiments on protoplast extracts showed two-order increase in current (from dark to light) under the same conditions (room temperature, humidity, and light). Compared with the photocurrent data from the plain buffer solution, the current was indeed primarily generated by the protoplast suspension when exposed to light, without minimal contribution from the buffer solution. The behavior of protoplast when exposed to light clearly shows that at 75 mV applied bias, a current of 338 nA is observed, which was around ~10 nA in case of dark conditions, the behavior of protoplast suspension and presence and absence of light is shown in Figure 3.14. If the structures are not around 100 micron or the structure observed is not similar to one shown, then cells were dead and there was no change in current between dark and light conditions.

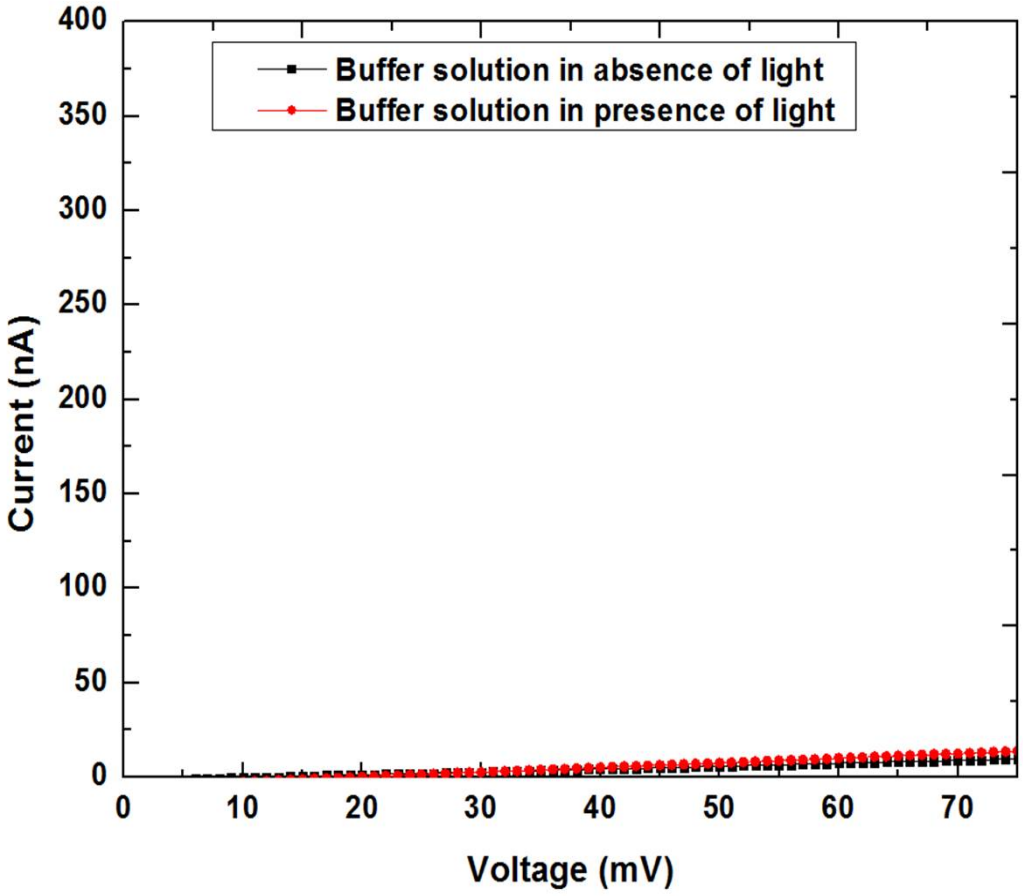

Figure 3.13 *I-V* plot showing conductivity through plain buffer solution in presence and absence of light.

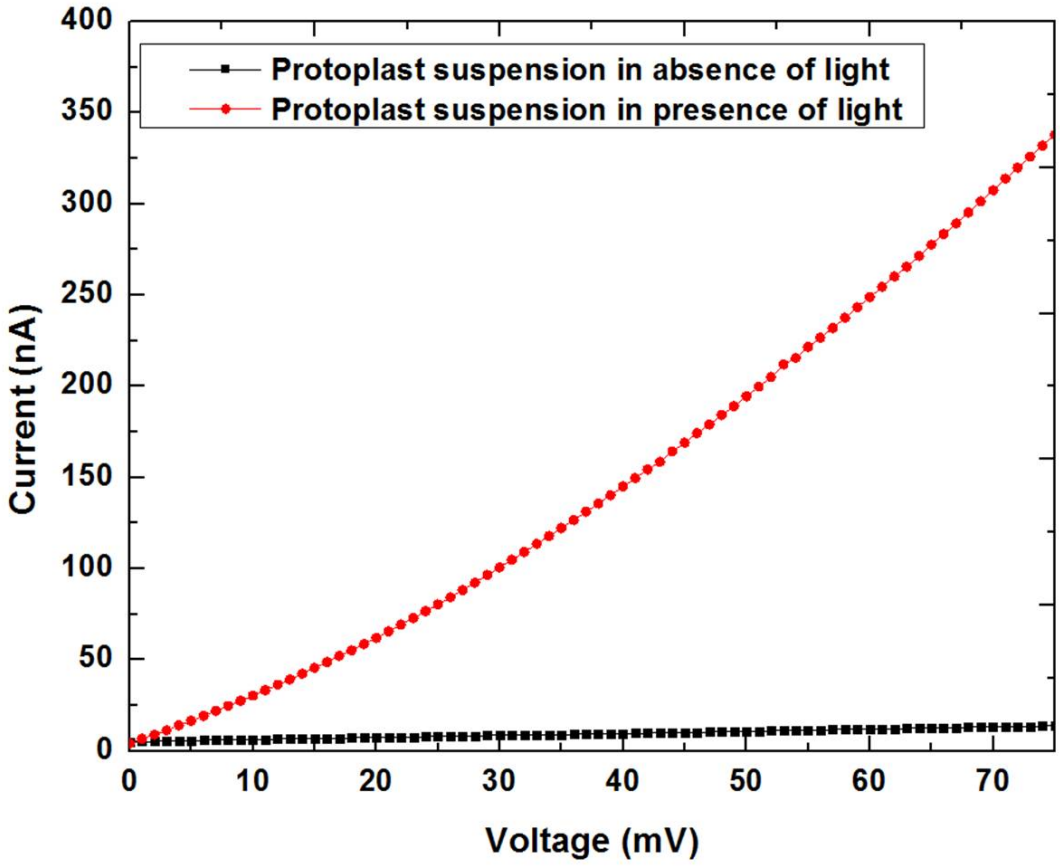

Figure 3.14 *I-V* plot showing behavior of the protoplast suspension in buffer solution under ramping voltage in presence and absence of light.

3.3.3 Optical Density Measurements

Figures 3.15 show the optical absorbance of the plain buffer solution and protoplast. The absorbance spectrum of protoplast demonstrated that the extracted protein complexes have very broad absorption band, which, we believe, enabled it to absorb light even in the visible-NIR region (600-1000 nm). The absorbance peaks of the protoplast suspension showed that UV light was absorbed at a greater quantity in the sample of Arabidopsis than in the buffer or cuvette. The calculated data for absorbance (optical density) indicated absorption bands at certain wavelengths which are shown in Table 3.1. These peaks indicate higher absorbance at certain wavelengths.

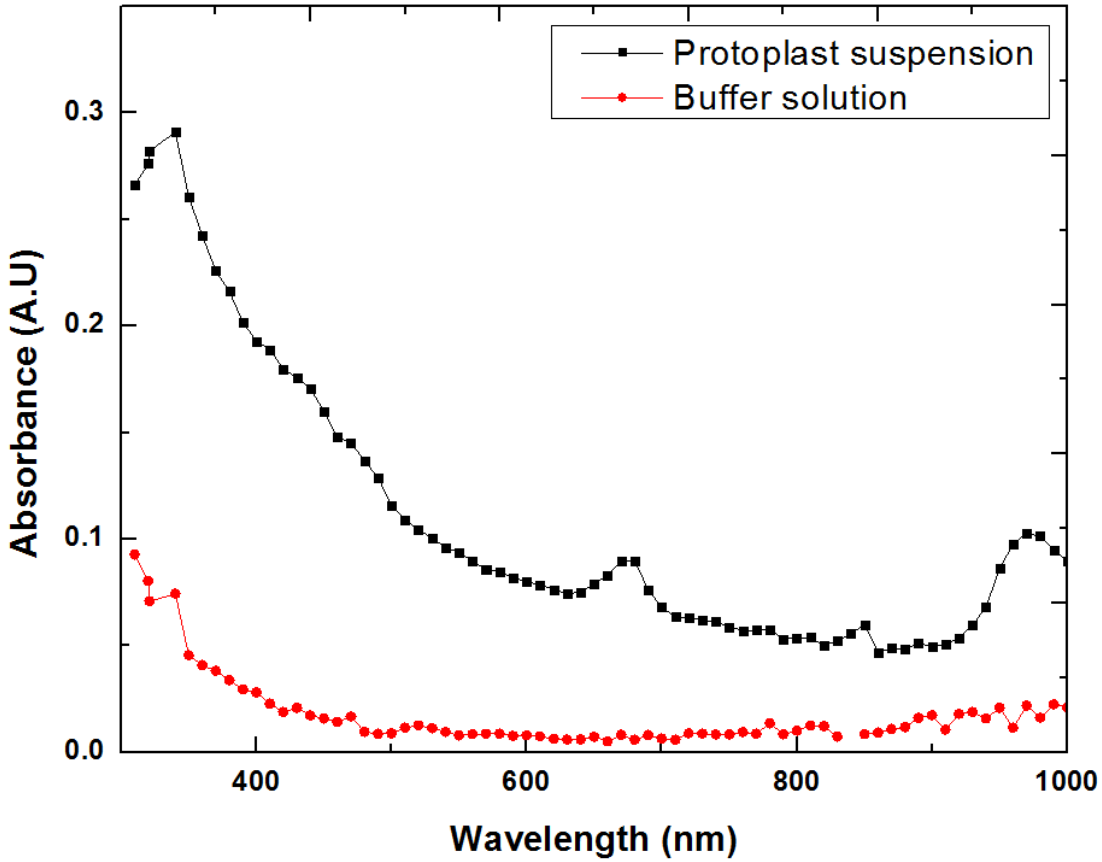

Figure 3.15 Optical absorbance spectrum of buffer solution and protoplast suspension at wavelength range was set from 300 to 1000 nm.

3.3.4 Statistical Analysis

For all the experiments (n=14), data were analyzed for mean ± standard deviation, the average current values ± standard deviations were calculated and graphed with an increment of 5 mV. The data indicated that the standard deviation in case protoplast suspension in absence of light was ± 0.34 (R^2 = 0.987) and in presence of light standard deviation was ± 0.33 (R^2 = 0.998). The standard deviation for buffer solution was higher than that of protoplast suspension. In absence of light buffer solution had standard deviation of ~ ± 8.46 (R^2 = 0.910) and it was ± 6.45 (R^2 = 0.947) in presence of light. Figure 3.16 Figure 3.17 shows the mean values ± standard deviation of current generated at different intervals of protoplast suspension in absence and presence of light. Figure 3.18 and Figure 3.19 shows the mean values of

current generated at different intervals and standard deviations of buffer solution in presence and absence of light. The average of current values at specific voltages, ranging from 0 to 75 mV with an increment of 5 mV, with increase in current with standard deviations is shown in Table 3.3.

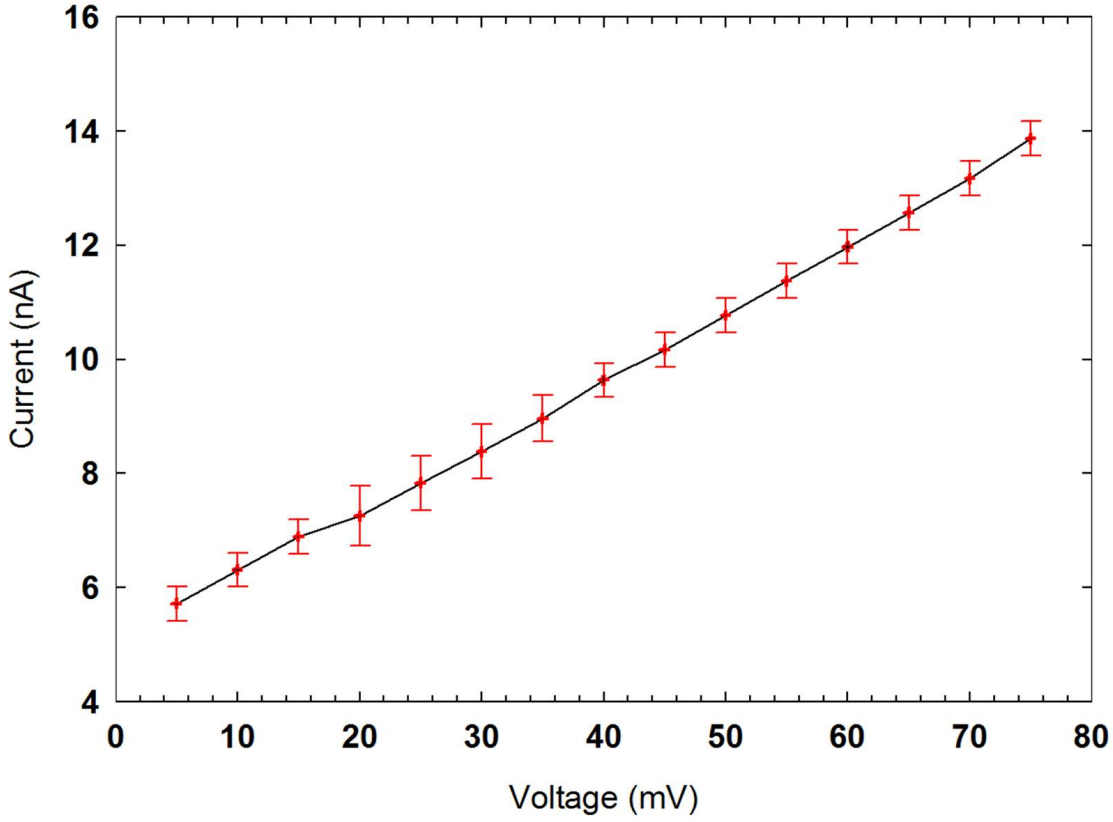

Figure 3.16 Mean ± standard deviation of current through protoplast suspension in absence of light. The data were collected from 14 independent experiments

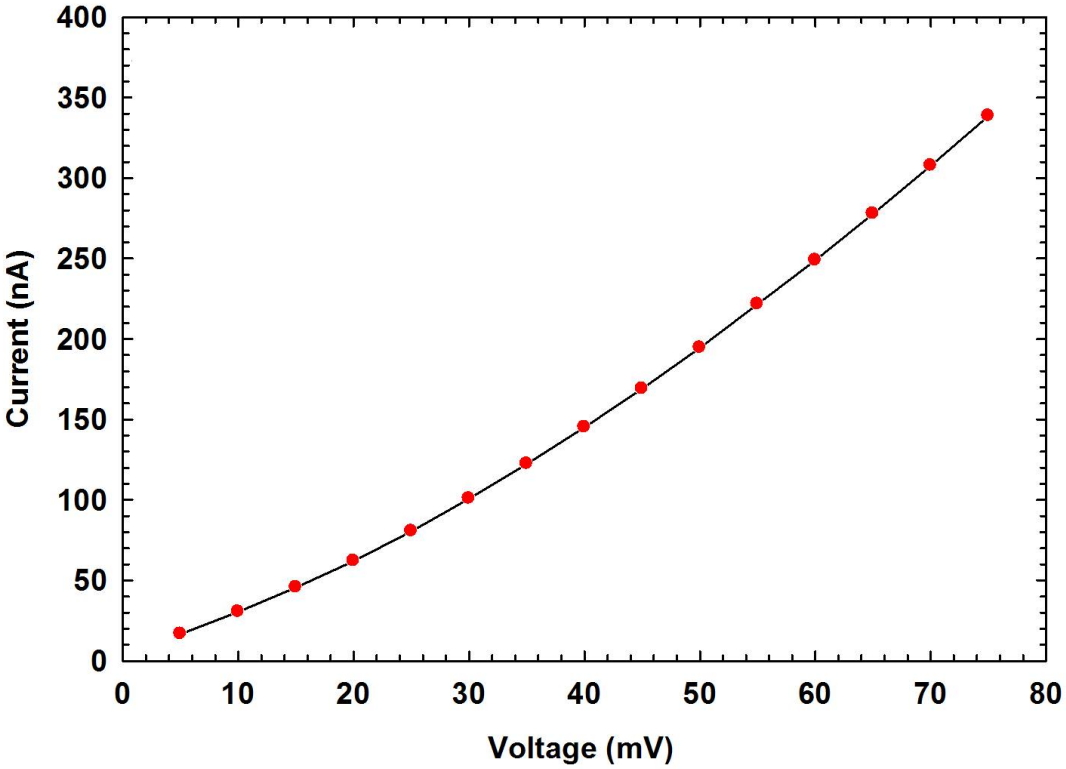

Figure 3.17 Mean ± standard deviation of current through protoplast suspension in presence of light. The data were collected from 14 independent experiments. The standard deviation is very small to be distinguished.

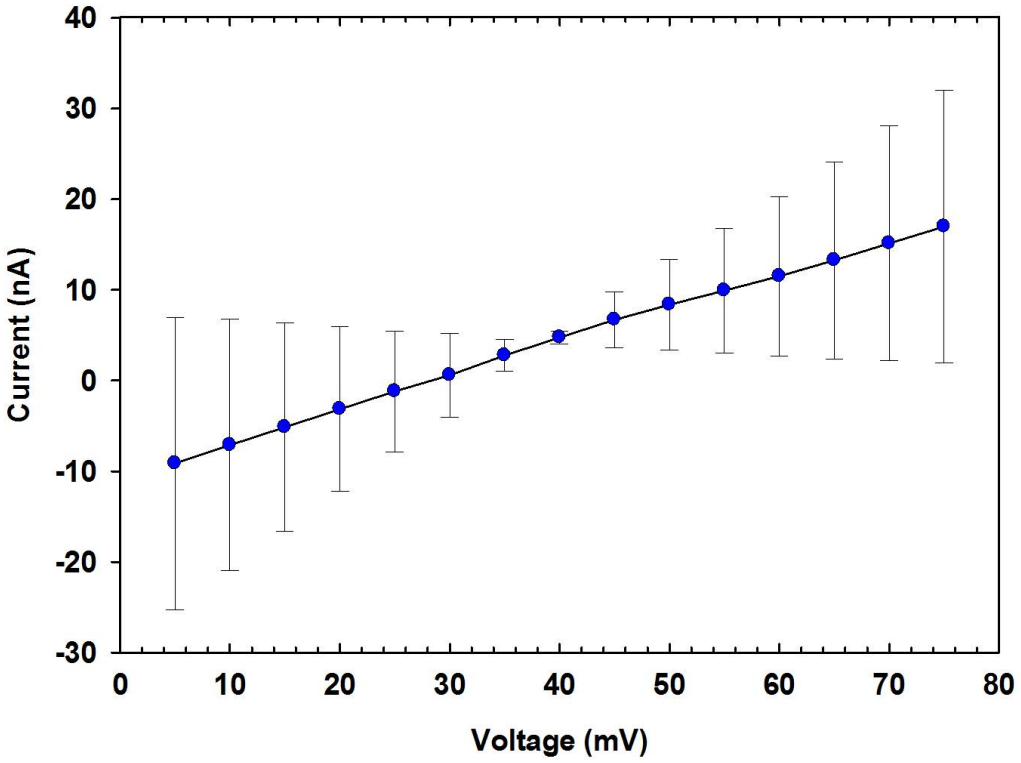

Figure 3.18 Mean ± standard deviation of current through buffer solution in absence of light. The data were collected from 14 independent experiments.

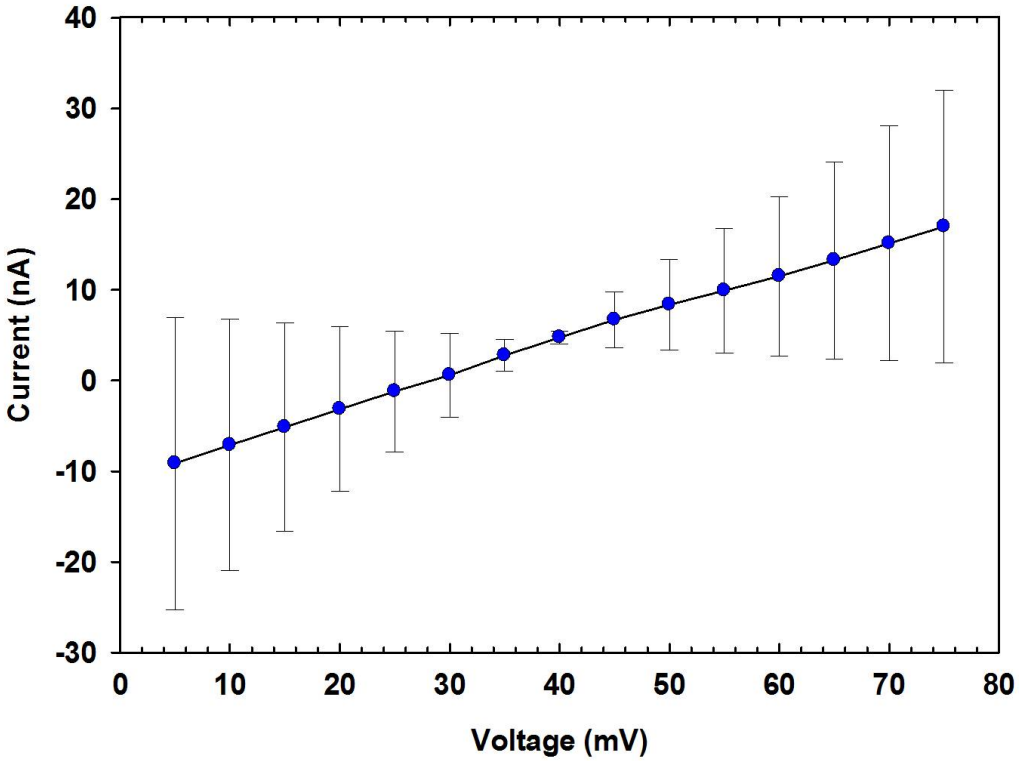

Figure 3.19 Mean ± standard deviation of current through buffer solution in presence of light. The data were collected from 14 independent experiments

Table 3.3 Mean ± standard deviation of current from 14 experiments performed independently.

Voltage (mV)	Buffer solution in absence of light (nA)	Buffer solution in presence of light (nA)	Protoplast suspension in absence of light (nA)	Protoplast suspension in presence of light (nA)
0	-11.93 ± 18.40	-10.76 ± 9.01	4.74 ± 0.30	4.08 ± 0 .27
5	-9.14 ± 16.12	-8.50 ± 10.13	5.72 ± 0.30	16.60 ± 0.2 7
10	-7.11 ± 13.86	-6.66 ± 11.05	6.31 ± 0.30	30.40 ± 0.2 7
15	-5.15 ± 11.47	-5.26 ± 11.00	6.89 ± 0.52	45.60 ± 0. 27
20	-3.16 ± 9.08	-3.77 ± 10.40	7.25 ± 0.48	62.00 ± 0.2 7
25	-1.20 ± 6.68	-2.23 ± 9.48	7.83 ± 0.48	80.44 ± 0.30

Table 3.3 – *Continued*

30	0.60 ± 4.60	-0.57 ± 8.36	8.38 ± 0.41	100.75 ± 0.30
35	2.77 ± 1.74	1.16 ± 7.06	8.96 ± 0.30	122.35 ± 0.30
40	4.75 ± 0.72	2.89 ± 5.72	9.63 ± 0.30	145.05 ± 0.30
45	6.70 ± 3.09	4.61 ± 4.36	10.17 ± 0.30	169.05 ± 0.30
50	8.36 ± 5.00	6.48 ± 2.59	10.77 ± 0.30	194.55 ± 0.30
55	9.928 ± 6.85	8.37 ± 0.95	11.37 ± 0.30	221.65 ± 0.30
60	11.50 ± 8.80	10.21 ± 1.11	11.97 ± 0.30	248.95 ± 0.30
65	13.27 ± 10.86	12.25 ± 2.98	12.57 ± 0.30	277.82 ± 0.45
70	15.12 ± 12.96	14.17 ± 4.81	13.17 ± 0.30	307.73 ± 0.46
75	16.98± 15.07	16.15 ± 6.80	13.87 ± 0.30	338.59 ± 0.60

3.4 Discussion

The results from *I-V* measurements indicated that the change in conductance of the buffer solution from dark to light was almost negligible compared to the change in the conductance of protoplast suspension in the presence of light. When protoplast suspension is exposed to light, photons are absorbed by protein complexes generating bound electron-hole pair (exitons) rather than free charges. These excitons which carry energy but no net charge diffuse through the solution and are dissociated into electrons and holes possibly when they reach the electrodes. These charges are collected at the respective electrodes - holes at anode and electrons at cathode, and are injected into an external circuit, resulting in an increase of output current [30]. Ideally all photogenerated excitons should reach a dissociation site in order to have maximum quantum efficiency. Their diffusion length should be large enough to reach the dissociation site otherwise they would recombine without contributing to the output current and thus photons are wasted. Exciton diffusion ranges in polymers and pigments are usually

around 10 nm [30, 31]. Therefore, excitons generated close to electrodes contribute to the total output current [30]. Secondly, excitons and charge transport usually need to hop from molecule to molecule in an organic material.

Closely packed molecules provide rapid exciton transport channels due to more intermolecular overlap and the dense packing of molecules also promotes the absorption coefficient [32]. Hence, as shown in Figures 3.13 and Figure 3.14 it can be concluded that light triggers a rapid sequence of events that include absorption of photons, generation and diffusion of excitons, charge separation and collection; resulting into a significant increase in the output current. Thus, the photosynthesis process can be efficiently used with our simple system to convert solar energy to electrical energy. These experiments were repeated multiple times to confirm this phenomenon with similar results. The theory behind this behavior of protoplast is that the absorption of light by the chloroplast present in protoplasts promotes the electrons to the higher energy level, in which electrons are repositioned in spatial and energy coordinates. The charge left behind is chemically oxidized, once the electron is reduced [33]. In any photosynthesis process, chloroplast plays a key role in capturing the photons and converting them to electrical energy.

The absorbance peaks of the protoplast suspension, shown in Figure 3.15, show that UV light is being absorbed at a greater quantity in the sample of *Arabidopsis* (~49 %) than as compared with buffer solution (~19 %) that confirms the presence of protoplast in the sample. The maximum absorbance represented by a peak of 340 nm concludes that cryptochromes are the primary UV absorber. In the mean time, absorption by phytochromes can be represented by the peak of 669 nm. Also, it was predicted that the buffer solution should behave differently at beginning because the current already stored in the solution requires some time to stabilize before it can act on voltage supplied. Statistical analysis confirmed this prediction for buffer solution, as shown in Table 3.3, the there was larger deviation in buffer solution as compared to

protoplast suspension. The protoplast suspension showed very small deviation, almost negligible, in absence of light and even smaller deviation in presence of light.

3.5 Conclusion

The results clearly indicate that plant protoplasts can be an efficient, environmental friendly, cheaper alternate for energy needs. Though there are certain limitations such as integration of biomolecular complexes in solid state electronic devices and low quantum efficiency, yet low band gap (less than 1.1 eV) makes plants and photosynthetic bacteria the best viable option for better harvesting of sunlight that can lead to enhanced efficiency of organic solar cells. It is safe to conclude that exposure of protoplast to light cause a series of events including absorption of photon's exciton generation, exciton dissociation, and hence a collection of charges that results in an increase in the net current output.

Utilizing protoplasts as a natural and instant energy source can greatly impact our rapidly growing world, by providing natural energy. As protoplasts absorb UV light, it is chemically converted into energy; this energy can be harnessed and used for many electrical innovations in the future. In the past few decades a lot of work has focused on various applications of photosynthetic proteins in technology, ranging from light induced electron transfer, sensing of herbicides, hydrogen production etc [2-5]. As protoplasts produce energy that can be stored for long periods of time by providing the required nutrients, protoplasts can be integrated in new class of solar panels that can prevent electrical shortages.

CHAPTER 4

FUTURE WORK

As discussed in earlier chapter 2.1.1, green sulfur bacteria (GSB) has markedly different photosynthetic thrust cross – cut two goals of electrical generation and Hydrogen storage. It is mostly present in depth of the lake where sunlight hardly reaches. It contains BChl-a and BChl-b having a ratio to the reaction center greater than other chlorosomes and of purified fraction of cytoplasmic membrane. Purple and GSB require light as an energy source along with suitable electron donor such as hydrogen sulfide. Much of the work has been done on Lake Species, in most lakes light of blue to yellow green wavelength band dominates at the depth. The majority of species in these habitats have different physiological and molecular basis of their obviously disadvantaged conditions [34]. The special property of *Chlorobium limicola* is that it is capable of growing at lower light intensities than other phototrophic bacteria [35]. The structure of *Chlorobium limicola* contains rod shaped structures that works as antennas which are capable of capturing sunlight and transferring it to the reaction center. In the reaction center this sunlight is then converted in to work energy. The rod elements from *Chlorobium limicola*, with the diameter of ~ 10nm, can be extracted and arranged according to the fabrication design discussed in Section 4.1.

4.1 Device Fabrication

As the future work, the protoplast from *Chlorobium limicola* can be isolated using similar method used for isolation of protoplast from Arabidopsis explained above. After isolation it should be inspected for presence of healthy cells. The solution will be integrated on a photo cell, using PDMS as a carrier / container for solution, between gold and Indium Tin Oxide (ITO) electrodes. The construction of the cell will include deposition of tin (<1000 Å) layer of amorphous organic semiconductor [C_{60}] between the photosynthetic center (the bacterial center

an top metal contact (Au); half inch ITO coated with glass slide as substrate with ITO serving as the bottom electrode. After the reaction center is assembled on to gold, the organic semiconductor layer and top layer will be sandwiched together. The fictionalization of ITO/Au will be done with surface fictionalization techniques described in literature [4, 36-39].

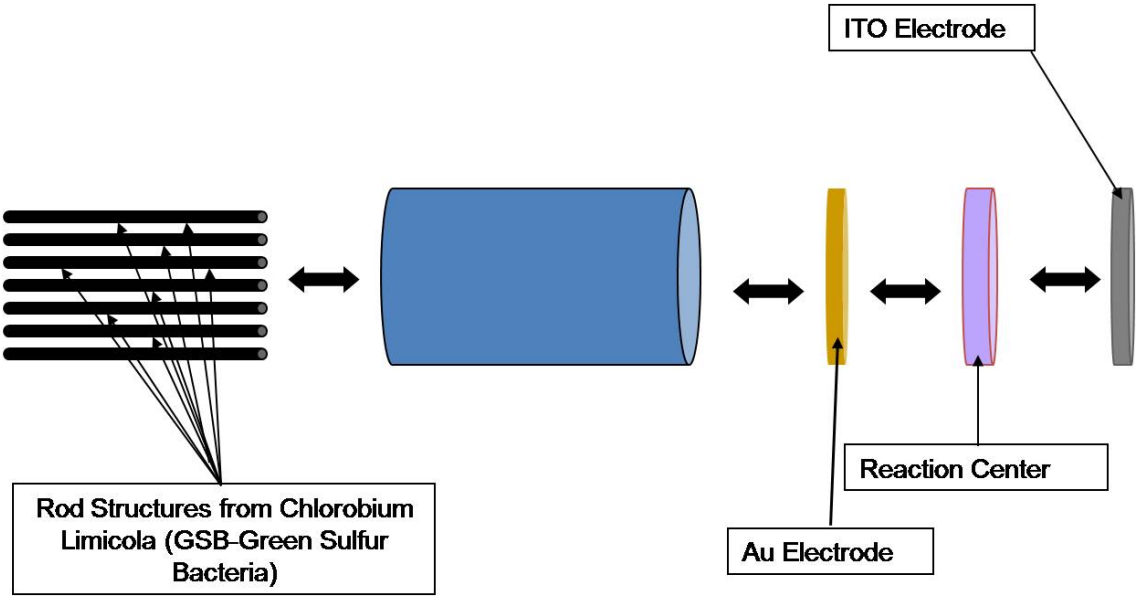

Figure 4.1 Schematic showing possible integration with extracted rod structures from *Chlorobium limicola*.

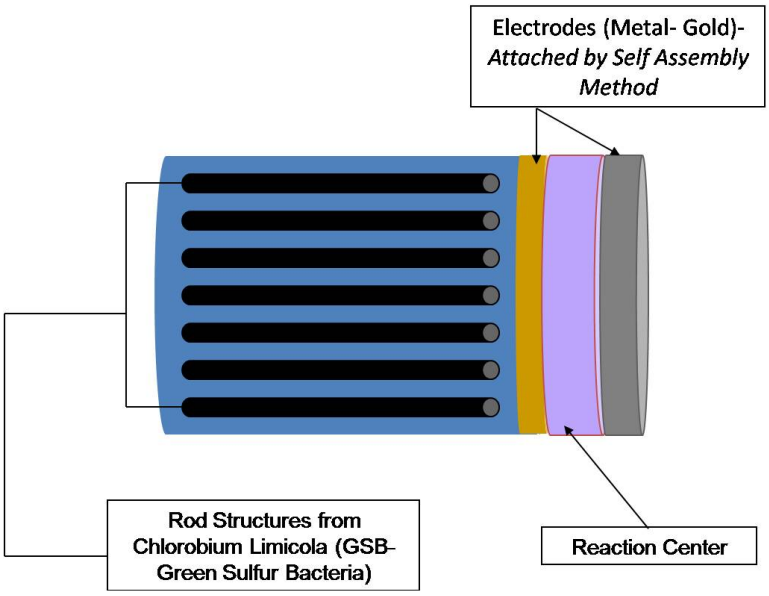

Figure 4.2 Components of solar cell integrated on to channel.

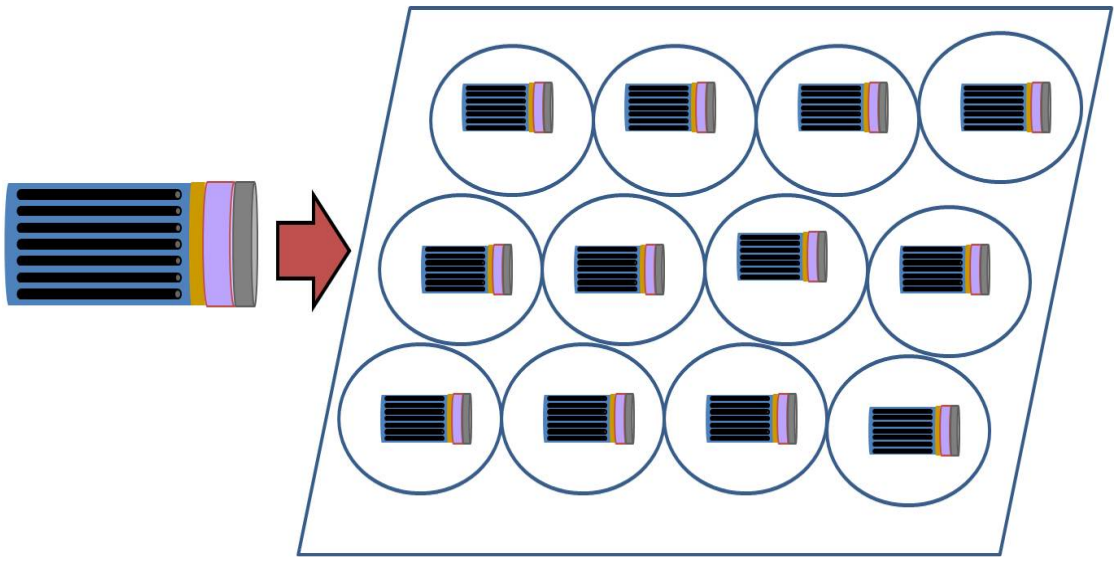

Figure 4.3 Layers can be added, combining single solar cell to increase the output of the device.

As shown in the Figure 4.3, the solar cell design can be expanded by combining a single working solar cell on a bigger scale. The energy converted by the solar cells can be used in many areas. It is expected that the future work discussed will have impacts on other areas of clean energy research like biofuels production. It can be used in the conversion of solar energy to chemical energy which is a major direction for cheap and clean development of fuel. Optimal design of bioreactors can provide unprecedented gains in efficiency.

APPENDIX A

PROTOPLAST ISOLATED FROM *ARABIDOPSIS* AT DIFFERENT DAYS

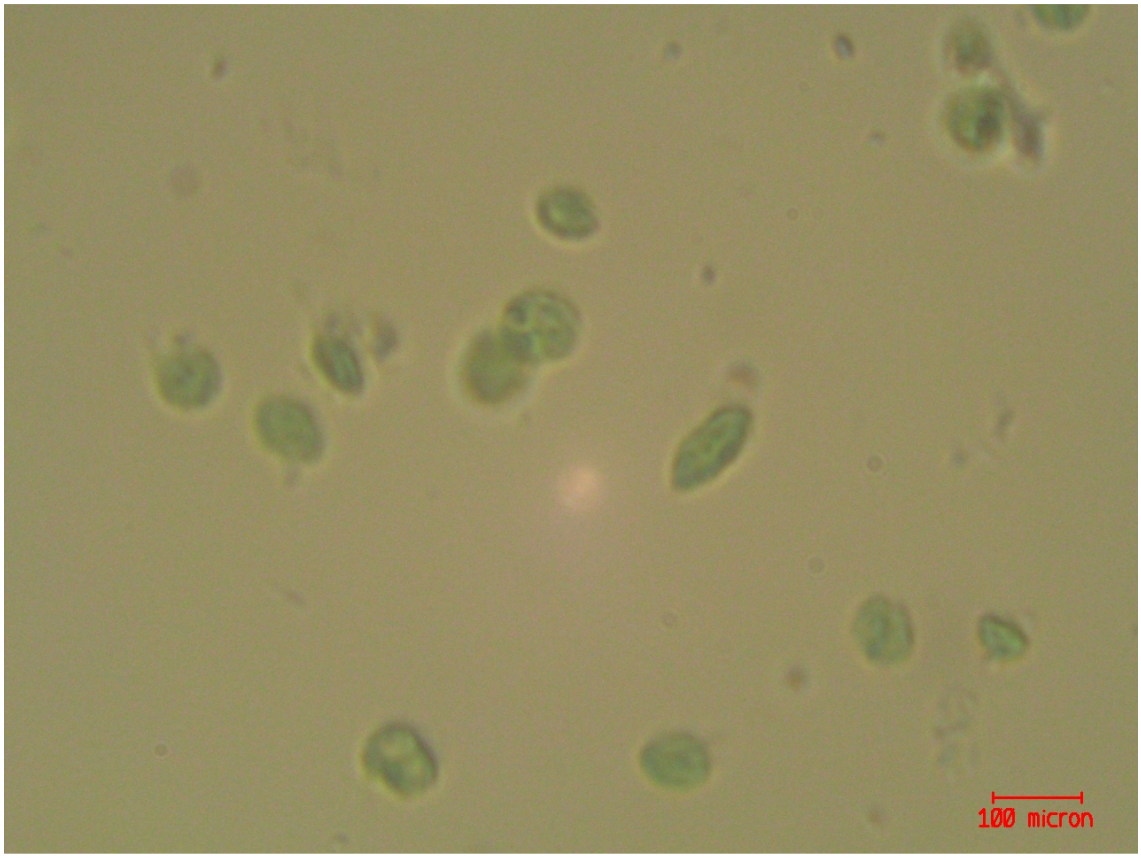

Figure A.1 Protoplast extracted from *Arabidopsis*, the green and round – oval shaped structures in the figure, image was the same day extraction was performed (Day 1).

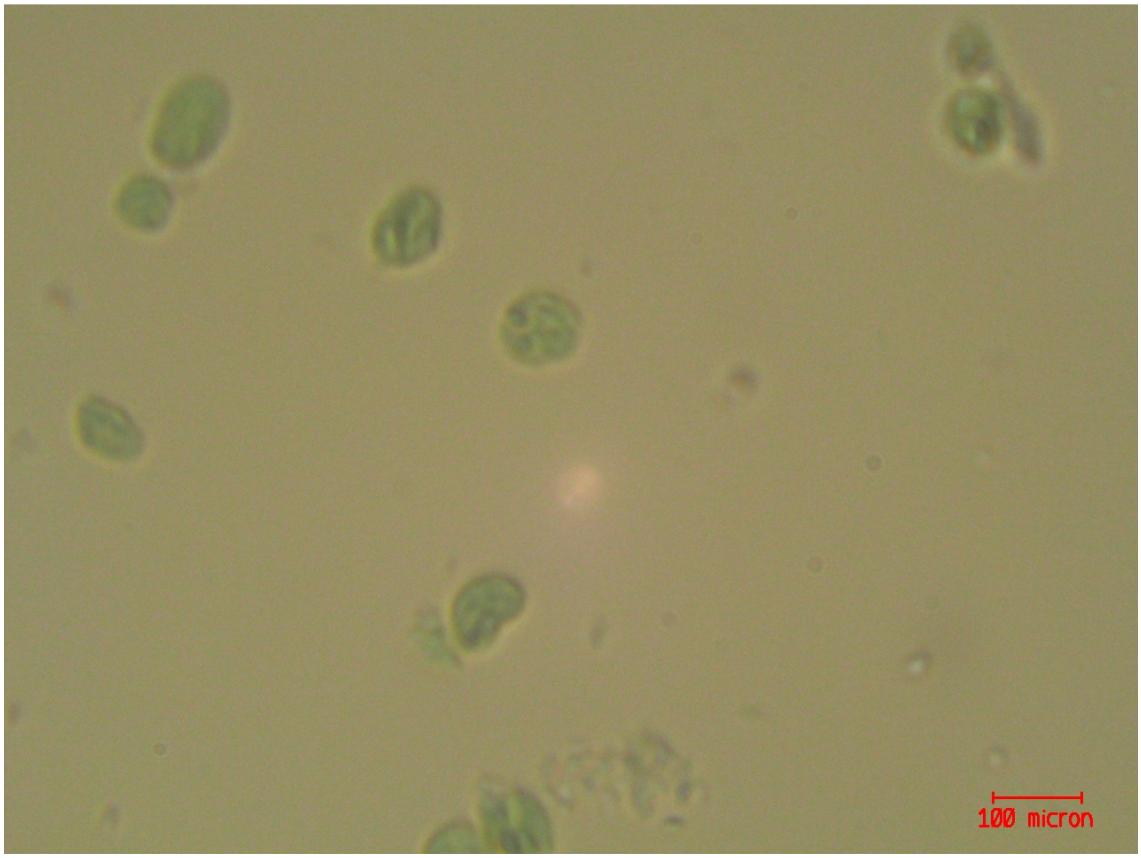

Figure A.2 Protoplast extracted from *Arabidopsis*, the green and round – oval shaped structures in the figure (Day 3).

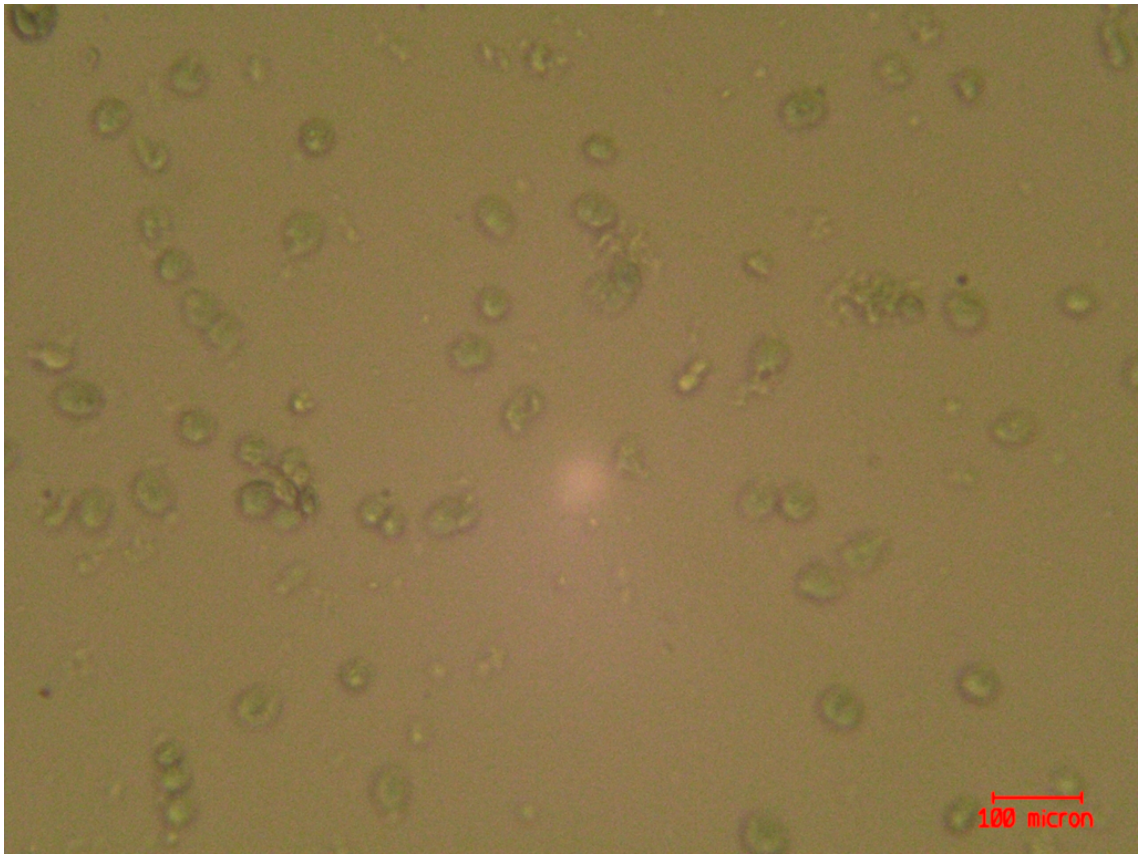

Figure A.2 Protoplast extracted from *Arabidopsis*, the green and round – oval shaped structures in the figure (Day 5).

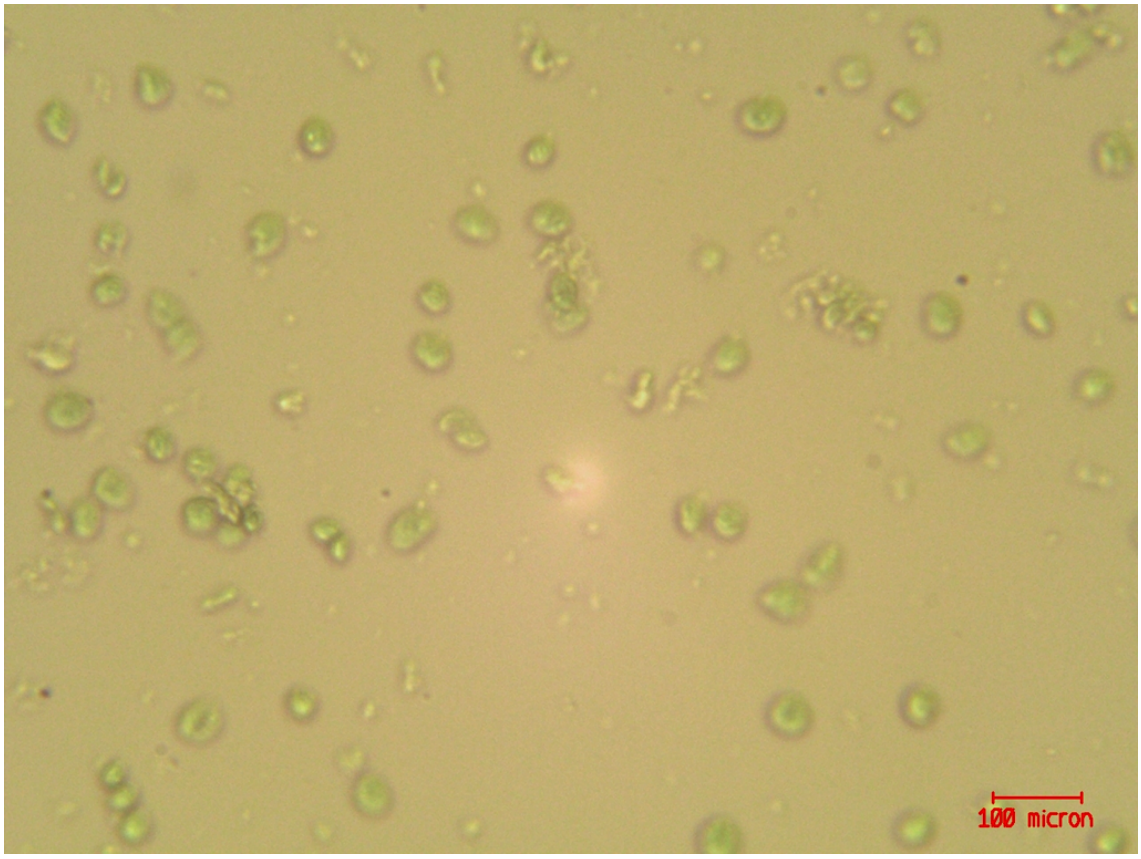

Figure A.3 Protoplast extracted from *Arabidopsis*, the green and round – oval shaped structures in the figure (Day 7).

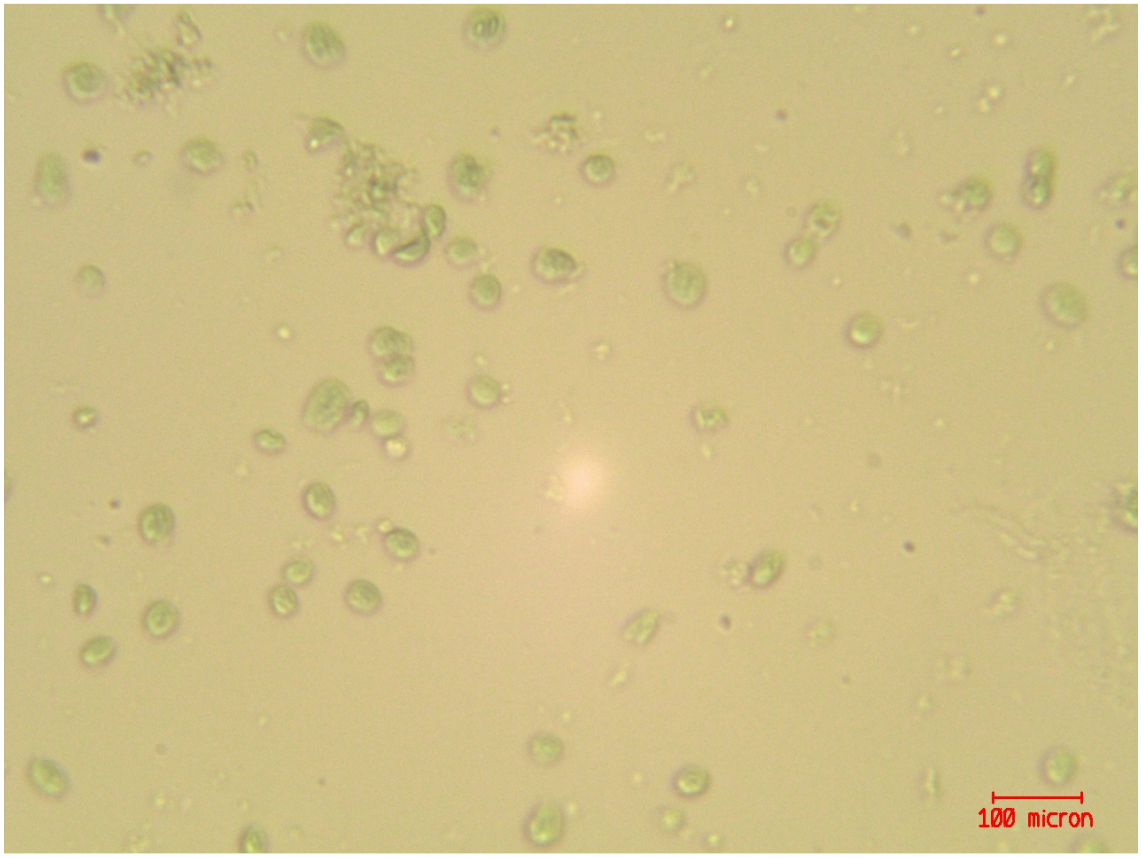

Figure A.4 Protoplast extracted from *Arabidopsis*, the green and round – oval shaped structures in the figure (Day 9).

APPENDIX B

EQUIPMENT USED FOR MEASUREMENTS

Figure B.1 Axopatch (Axon 200B), a patch clamp used for measurements.

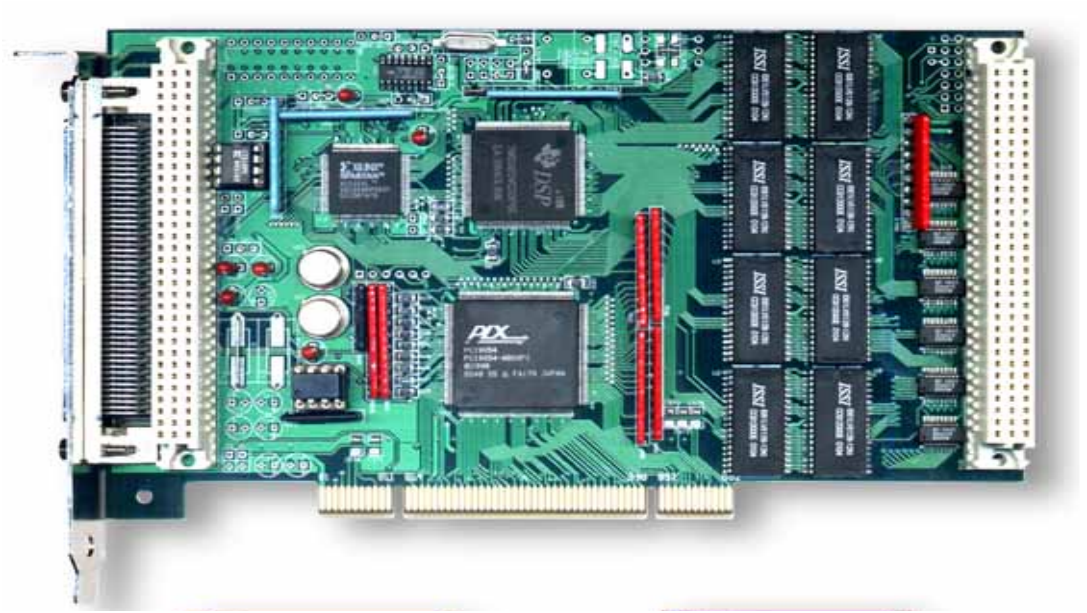

Figure B.2 NI – 6070E card which converts analog signal to digital and vice versa.

Figure B.3 National Instruments (NI) data acquisition card 68 used to supply voltage and read current produced.

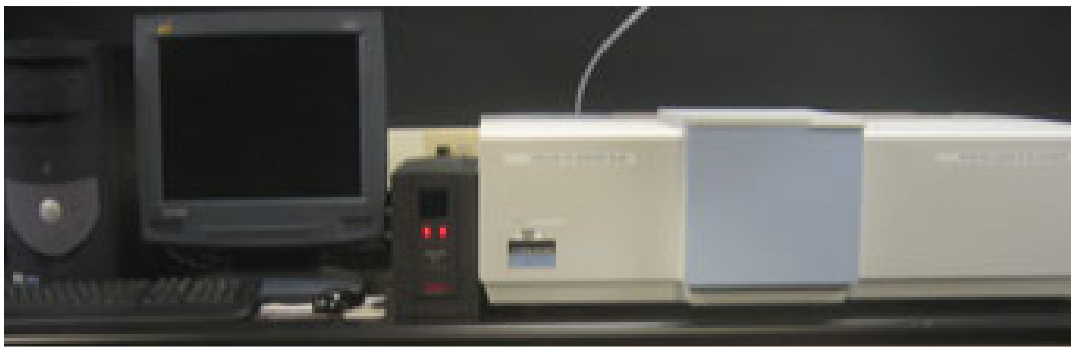

Figure B.4 Setup for Perkin Elmer UV/VS/NIR spectrometer, used for optical density measurements.

REFERENCES

1. Haehnel, W. and H.J. Hochheimer, *On the current generated by a galvanic cell driven by photosynthetic electron transport.* Journal of Electroanalytical Chemistry and Interfacial Electrochemistry, 1979. **104**: p. 563-574.
2. Esper, B., A. Badura, and M. Rogner, *Photosynthesis as a power supply for (bio-) hydrogen production.* Trends in plant science, 2006. **11**(11): p. 543-549.
3. Giardi, M.T. and E. Pace, *Photosynthetic proteins for technological applications.* Trends in biotechnology, 2005. **23**(5): p. 257-263.
4. Ho, D., et al., *Fabrication of biomolecule–copolymer hybrid nanovesicles as energy conversion systems.* Nanotechnology, 2005. **16**: p. 3120.
5. Touloupakis, E., et al., *A multi-biosensor based on immobilized Photosystem II on screen-printed electrodes for the detection of herbicides in river water.* Biosensors and Bioelectronics, 2005. **20**(10): p. 1984-1992.
6. M. Baldo and Das, R., *Photovoltaic devices using photosynthetic protein complexes.* 2004.
7. Tiedje, T., et al., *Limiting efficiency of silicon solar cells.* Electron Devices, IEEE Transactions on, 1984. **31**(5): p. 711-716.
8. Green, M.A., *Solar cells: operating principles, technology, and system applications.* Englewood Cliffs, NJ, Prentice-Hall, Inc., 1982. 288 p., 1982. **1**.
9. Melis, A., *Solar energy conversion efficiencies in photosynthesis: Minimizing the chlorophyll antennae to maximize efficiency.* Plant Science, 2009. **177**(4): p. 272-280.
10. Sundström, V.,Light in elementary biological reactions, Progress in quantum electronics, 2000. 24(5):p. 187-238.

11. Hoff, A.J. and J. Deisenhofer, *Photophysics of photosynthesis. Structure and spectroscopy of reaction centers of purple bacteria.* Physics reports, 1997. **287**(1-2): p. 1-247.

12. Beekman, L.M.P., et al., *Characterization of the light-harvesting antennas of photosynthetic purple bacteria by Stark spectroscopy. 2. LH2 complexes: Influence of the protein environment.* The Journal of Physical Chemistry B, 1997. **101**(37): p. 7293-7301.

13. Terazono, Y., et al., *Multiantenna Artificial Photosynthetic Reaction Center Complex.* The Journal of Physical Chemistry B, 2009. **113**(20): p. 7147-7155.

14. Barber, J. Biological solar energy. *Philosophical Transactions of the Royal Society A: Mathematical, Physical and Engineering Sciences*, 2007, 365(1853), 1007.

15. Ametller, C.A., E. Montesinos, and R. Guerrero, *Field studies on the competition between purple and green sulfur bacteria for available light (Lake Siso, Spain)*. 1980: Dr. W. Junk.

16. Herbert, R.A. and A.C. Tanner, *The isolation and some characteristics of photosynthetic bacteria (Chromatiaceae and Chlorobiaceae) from Antarctic marine sediments.* Journal of Applied Microbiology, 1977. **43**(3): p. 437-445.

17. Kirk, J.T.O., *Spectral distribution of photosynthetically active radiation in some south-eastern Australian waters.* Marine and Freshwater Research, 1979. **30**(1): p. 81-91.

18. G. Hauska, T.S., Herve Remigy, and G. Tsiotis, *The Reaction Center of Green Sulfur Bacteria* Bioenergetics, 2001. **1507**(1-3): p. 260-277.

19. Haehnel, W. and H.J. Hochheimer, *On the current generated by a galvanic cell driven by photosynthetic electron transport.* Journal of Electroanalytical Chemistry, 1979. **104**: p. 563-574.

20. B. R, G., *Solution to Light Harvesting Problem:Mix, match, and duplicate., in Photosynthesis:Mechanisms and Effects.* 1999: p. 587-590.

21. Nechushtai R, E.A., Cohen Y and Klein J, *Introduction to Photosystem I :Reaction center function, composition and structure, in Oxygenic Photosynthesis: The light Reaction.* 1996: p. 289-311.

22. Das, R. *Photovoltaic Devices Using Photosynthetic Protein Complexes*. (Massachusetts Institute of Technology, Dept. of Electrical Engineering and Computer Science, 2004).

23. Melis, A., *Spectroscopic methods in photosynthesis: photosystem stoichiometry and chlorophyll antenna size.* Philosophical Transactions of the Royal Society of London. B, Biological Sciences, 1989. **323**(1216): p. 397.

24. Somerville, E.M.M.a.C.R., *Arabidopsis.* Cold Spring Harbor Laboratory Pr., 1994.

25. McDonald, J.C., P. Sebastien, and B. Armstrong, *Radiological survey of past and present vermiculite miners exposed to tremolite.* British journal of industrial medicine, 1986. **43**(7): p. 445.

26. Pandey, S., Wang, X.Q., Coursol, S.A. and Assmann, S.M. Preparation and applications of Arabidopsis thaliana guard cell protoplasts. *New phytologist*, 2002, 153(3), 517-526.

27. Miedema, H. and Assmann, S.M. A membrane-delimited effect of internal pH on the K+ outward rectifier of Vicia faba guard cells. *Journal of Membrane Biology*, 1996, 154(3), 227-237.

28. Assmann, S.M. and Romano, L. Secondary messenger regulation of ion channels/plant patch clamping. *Methods in enzymology*, 1999, 294, 410.

29. Ingle Jr, J.D. and Crouch, S.R. Spectrochemical analysis. *Englewood Cliffs, NJ*, 1988, 106.

30. J.J.M. Halls, K.P., R.H. Friend, S.C. Moratti, and A.B. Holmes. Exciton Diffusion and dissociation in a poly(p-phenylenevinylene)/C-60 heterojunction photovoltaic cell. *Applied Physics Letters*, 1996, 22(68), 2.

31. Choong, V., Park, Y., Gao, Y., Wehrmeister, T., Müllen, K., Hsieh, B.R. and Tang, C.W. Dramatic photoluminescence quenching of phenylene vinylene oligomer thin films upon submonolayer Ca deposition. *Applied Physics Letters*, 1996, 69, 1492.

32. Kasap, S.O. Optoelectronics and photonics principles and practices.

33. Beekman, L.M.P., Frese, R.N., Fowler, G.J.S., Picorel, R., Cogdell, R.J., van Stokkum, I.H.M., Hunter, C.N. and van Grondelle, R. Characterization of the light-harvesting antennas of photosynthetic purple bacteria by Stark spectroscopy. 2. LH2 complexes: influence of the protein environment. *J. Phys. Chem. B*, 1997, 101(37), 7293-7301.

34. Overmann, J. Diversity and ecology of phototrophic sulfur bacteria. *Microbiology Today*, 2001, 28, 116-119.

35. Biebl, H. and Pfennig, N. Growth yields of green sulfur bacteria in mixed cultures with sulfur and sulfate reducing bacteria. *Archives of Microbiology*, 1978, 117(1), 9-16.

36. Das, R., Kiley, P.J., Segal, M., Norville, J., Yu, A.A., Wang, L., Trammell, S.A., Reddick, L.E., Kumar, R. and Stellacci, F. Integration of photosynthetic protein molecular complexes in solid-state electronic devices. *Nano Letters*, 2004, 4(6), 1079-1083.

37. Escalante, M., Maury, P., Bruinink, C.M., Werf, K., Olsen, J.D., Timney, J.A., Huskens, J., Hunter, C.N., Subramaniam, V. and Otto, C. Directed assembly of functional light harvesting antenna complexes onto chemically patterned surfaces. *Nanotechnology*, 2008, 19, 025101.

38. Ogawa, M., Shinohara, K., Nakamura, Y., Suemori, Y., Nagata, M., Iida, K., Gardiner, A.T., Cogdell, R.J. and Nango, M. Self-assembled monolayer of light-harvesting 1 and reaction center (LH1-RC) complexes isolated from Rhodospirillum rubrum on an amino-terminated ITO electrode. *Chemistry Letters*, 2004, 33(6), 772-773.

39. Frolov, L., Rosenwaks, Y., Carmeli, C. and Carmeli, I. Fabrication of a photoelectronic device by direct chemical binding of the photosynthetic reaction center protein to metal surfaces. *Advanced Materials*, 2005, 17(20), 2434-2437.

BIOGRAPHICAL INFORMATION

Ahmed Shahid became Member of Phi Theta Kappa in 2004, Member of Mu Alpha Theta in 2005, and Member of BMES in 2009. He was awarded with Travel Grant from EE & BME Department in 2009, Travel Grant from EE & BME Department in 2010, Consortium for Nanomaterials for Aerospace Commerce and Technology Student Travel Grant (CONTACT) since Fall 2010 – Present, Phi Theta Kappa Honors Scholarship 2007 – 2010, Good Standing Scholarship U. T. Arlington from Spring 2007 – Fall 2011, Good Standing Scholarship from Electrical Engineering Department in Fall 2010. He was also selected for Phi Theta Kappa's President Honor Roll List with Excellence in Academia in 2005, 2006, and 2009, and Outstanding Academic Performance, Spring 2008 – Spring 2011.

Shahid was born on September 4, 1983. Shahid completed his high school in Saudi Arabia and moved to Michigan for his higher education as Electrical Engineer. In 2004, Shahid moved to Texas completed his Associate Degree in Applied Science May 2006 and Associate of Science in Mathematics in May 2007 from North Lake College, Irving, Texas and moved to University of Texas at Arlington in 2008.

He has worked for North Lake College as LAN – WAN Support Specialist III. Currently he is working under Dr. Samir Iqbal on his Masters in Biomedical Engineering. He is been working with Dr. Samir Iqbal since February 2009 as research assistant and his previous and current interests includes designing devices and chips that should perform their operations uniquely, precisely and closed to perfection using natural resources. His future research plan includes: Isolation and reduction of Tumor cells using a unique method designed in laboratory.